#26

U.S. Department
of Transportation

**Federal Railroad
Administration**

POWER TRANSFER TO HIGH SPEED VEHICLES

DOT/FRA/NMI-92/03

July 1992
Final Report

Technical Report Documentation Page

1. Report No. DOT/FRA/NMI-92/03	2. Government Accession No.	3. Recipient's Catalog No.
4. Title and Subtitle Power Transfer to High Speed Vehicles		5. Report Date July 1992
		6. Performing Organization Code 30233
7. Author(s) David Cope, Paul Chambers		8. Performing Organization Report No. DOT-0044-FM-9352-535
9. Performing Organization Name and Address Foster-Miller, Inc. 350 Second Avenue Waltham, MA 02154-1196		10. Work Unit No. (TRAIS) N/A
		11. Contract or Grant No. DTFR53-91-C-00044
12. Sponsoring Agency Name and Address	U.S. Department of Transportation Federal Railroad Administration Office of Procurement Services 400 7th Street, S.W., Room 8222 Washington, DC 20590	13. Type of Report and Period Covered Final Report- July 1991-June 1992
		14. Sponsoring Agency Code N/A
15. Supplementary Notes	COTR: Mr. M. Coltman, Mr. R. Murphy U.S. Department of Transportation Transportation Systems Center Kendall Square Cambridge, MA 02142	

16. Abstract

This final report summarizes work performed in the assessment and analysis of power transfer techniques to high speed vehicles. The objectives of this research were to determine the optimum power transfer technique for two power levels at high speed and to prepare a preliminary design of the optimum power transfer technique. The power levels are "hotel" power (P ~ 100 kW) and drive power (P ~ 40 MW). This investigation was restricted to power transfer techniques of contact (brush) and non-contact (inductive) types.

It is recommended that power be transferred by air-core transformer action between the stationary guideway and the moving vehicle across the full air gap. The direct current power is inverted locally by semiconductor switches operating at 1 kHz. Power factor correction is performed by a capacitor on-board the vehicle. According to a design example, approximately 1 MW can be transferred per coil across the full air gap (100 mm) per meter of vehicle sidewall. Therefore, 40 MW can be transferred by coils on both sides of a 20 m vehicle.

The major advantage of this technique is non-contact high power transfer independent of vehicle speed. The overall economics of this technique are competitive with other systems. Moreover, this concept provides performance no other concept can provide at any price

17. Key Words power transfer, hotel power, drive power, contact and non-contact means, inductive coils		18. Distribution Statement Document is available to the U.S. public through the National Technical Information Service, Springfield Virginia, 22161	
19. Security Classif. (of this report) UNCLASSIFIED	20. Security Classif. (of this page) UNCLASSIFIED	21. No. of Pages 75	22. Price

Form DOT F 1700.7 (8-72) Reproduction of completed page authorized

TABLE OF CONTENTS

TABLE OF CONTENTS (Continued)

Section **Page**

LIST OF ILLUSTRATIONS

LIST OF TABLES

EXECUTIVE SUMMARY

ES.1 Introduction

Magnetically levitated transportation is being investigated as a method of transporting passengers and freight over relatively long distances (100 to 1,000 km) at relatively high speeds (135 m/s). Due to environmental and energy efficiency considerations the most viable Maglev options appear to be all-electric with the electric power being centrally generated, transmitted to the guideway and delivered to the vehicle. A typical high speed Maglev vehicle will require instantaneous power of 10 MW. This estimate is based upon an energy consumption of 980 J/passenger-kilometer (1), and 75 passengers per vehicle. Several such vehicles traveling as a unit (a "train") will, of course, require additional power. Transporting 600 passengers in an eight vehicle train could require up to 40 MW of instantaneous power. This estimate uses the fact that at steady speed most of the energy consumption is due to air drag, and, of course, several vehicles in a train reduce the air drag per vehicle.

Maglev transportation could be driven, at least in part, by power transfer techniques. Proven electric power transfer techniques are typically limited to low powers and/or low speeds. Significant exceptions to this statement include the high speed rail enterprises French Tres Grande Vitesse (TGV) (2) and German Inter-City Express (ICE) (3) and prototype Maglev efforts Japanese Railway (MLU002) (4) and German Transrapid (TR07) (5). Under special circumstances, these high speed rail systems have demonstrated high power transfer (~10 MW) at high speed (135 m/s = 480 kph = 300 mph). The Maglev systems have transferred smaller levels of power (100 to 250 kW) at 135 m/s (300 mph).

If any of the power transfer techniques utilized in the above mentioned systems were wholly adequate, the power transfer problem could be considered solved, with remaining tasks being optimization of the existing techniques. Unfortunately, all existing power transfer techniques suffer from disadvantages (discussed later) which makes the development of a new power transfer technique desirable.

As part of this research, we reviewed a large volume of relevant literature on power transfer techniques. In addition to articles in English, we reviewed articles in Japanese, German and French. This literature is discussed and referenced throughout the report and listed in the bibliography.

The power required by a Maglev system serves two basic purposes: "drive" and "hotel" power requirements. Drive power is the power required to propel the vehicle at high speed. Depending upon the specific design and speed, power requirements can easily exceed 10 MW per vehicle to overcome aerodynamic drag and to provide hill climbing power. For this study we considered power requirements up to 40 MW, representing a multivehicle train.

Hotel power is the power required to provide vehicle heating, ventilation, air conditioning (HVAC), lighting, and, if applicable, refrigeration for superconductors. Depending upon the system design, hotel power requirements typically amount to less than 250 kW/vehicle.

ES.2 Objectives

The objectives of this research were: firstly to determine the maximum practical power transferrable to a magnetically levitated (Maglev) vehicle traveling at high speed; and secondly, to develop a preliminary design of the optimum power transfer technique. We restricted our investigation of power transfer techniques to contact (brush) and non-contact (inductive) means.

In determining the optimum transfer technique, consideration was given to the following characteristics, among others: power regime, technical risk, safety of on-board or wayside personnel, electromagnetic interference, reliability, maintainability, vehicle weight impact, vehicle speed effects, sensitivity to traffic density, aerodynamic effects (drag and noise), esthetics, capital and operating costs, etc. A complete list of issues considered is given in subsection 2.2.

ES.3 Technology Issues

With regards to the actual transfer of power, the vehicle can be active and the guideway can be passive, or, conversely, the vehicle can be passive and the guideway can be active. The former situation is similar to present-day high speed electrified rail systems. In this case, the "guideway" is simply two well-aligned rails and the active vehicle propels itself down the track. Note that the existence of an intricate wayside high power delivery system delivering ~10 MW to the train does not disqualify the guideway from being identified as "passive."

High speed rail has made significant strides in developing high speed, high power transfer methods. In general, they rely upon contact means (brushes). For highest speeds and greatest powers, rail systems typically use an overhead high voltage catenary wire and on-board

pantograph for power collection. Unfortunately for power transfer, catenaries have unstable dynamic modes which are excited by high speed pantographs. On a test run, the French (TGV) have attained a maximum speed of 142 m/s (6) while transferring approximately 8 MW via a 25 kV, 50 Hz single phase ac, single catenary, system. The current is returned through the rails. The track and overhead equipment were specially tuned for the record setting run. While representing a significant milestone for steel-wheel-on-rail systems, to achieve such performance for routine service would require constant, costly "tuning" of the system. The performance demonstrates significant technology developments in the areas of catenary dynamics and brush materials.

Our recommended power transfer technique relies upon recent developments in power semiconductor devices. Section 3 describes the recommend approach in details.

ES.4 Technology Assessment Results

The power transfer concepts considered for this study include:

- Contact means via
  - Catenary/pantographs
  - Brushes on rigid rails
- Non-contact inductive energy transfer via
  - Harmonic frequencies generated by either the propulsion coils or the superconducting magnet (if applicable)
  - Dedicated power transfer coils.

The dynamics of high speed traversal of a catenary were studied (7,8) and the fundamental result was obtained that the catenary/pantograph system was able to provide approximately 10 MW at 143 m/s (320 mph) (9). Higher speed trains are discussed in the technical literature as theoretically possible (up to 200 m/s (450 mph) (10) with additional catenary and pantograph improvements, but discussions of greater power are not evident.

The issues with high speed catenary/pantograph power collection are:

- Pantograph aerodynamics
- Pantograph air-induced noise
- Electrical noise
- Catenary dynamics
- Mechanical design to maintain the required tension throughout temperature changes
- Dual collectors (at a minimum) are required for Maglev
- Pantograph and catenary wear rates.

Rigid rail power transfer was investigated and the basic result is that is it possible to transfer approximately 10 MW through rails. It should be noted that this accomplishment is nothing more than depositing the return current of the above cited catenary into the rails via the rolling contact of the train set. In this case there is a large contact force (660 kN) (11) and a large contact area so it would be surprising if it were not possible. Limiting our consideration to reasonably light contact forces we find the bifurcated result that the high speed operation of rails has been proven with a passive current collector (12,13) and power transfer of 2 to 5 MW has been proven at medium speeds.(14). This reference describes rotating wire brushes for current collection. It was found that high current collection was possible at reasonable brush wear rates.

Issues with a rigid rail power transfer system are:

- Voltage safety for personnel
- Power delivered
- Rail tracking mechanism required
- Brush and rail wear rates
- Dual contact collectors required for maglev appear inconsistent with magnetic levitation.

Two noteworthy studies of Maglev systems (15,16) have suggested contact means for high power transfer at high speed.

Non-contact power transfer via harmonic frequencies of a fundamental has been used with success by both the Japanese and German Maglev systems. This technique, by its very nature, relies upon recovering a fraction of the propulsive power for the transferred power so the overall magnitude of power transferred is limited at all speeds and is zero at standstill. External power to provide vehicle locomotion must be supplied from another source. Hence, harmonic frequency

power transfer is inherently incapable of providing the drive power for the vehicle.The Japanese power transfer system for the vehicle series designated MLU-00x relies upon harmonics of the passage of the superconductor over stationary horizontal ground coils embedded within the guideway. Approximately 100 kW (17) of power per vehicle is generated by this method when the drive power is 5 MW.

The German Maglev system relies upon power transfer from the propulsion coils in the slotted magnetic guideway. Approximately 250 kW (18) of power per vehicle is generated by this method.

ES.5 Proposed Power Transfer System

The new and recommended power transfer method is the following: power is transferred by air-core transformer action between the stationary guideway and the moving vehicle across the full air gap. To improve the efficiency the coils are designed to be large compared to the gap. The power is fed at dc and inverted locally by solid-state switches operating at 1 kHz in an H-bridge configuration. Power factor correction is performed by capacitors on-board the vehicle. As described in detail in Section 3, for the system analyzed, up to approximately 40 MW can be transferred across the full air gap (100 mm). The number of coils per vehicle is variable, allowing considerable design flexibility: "power transfer" vehicles, somewhat similar in concept to locomotives, can be designed to acquire the total train power (Figure 1), or, conversely, each vehicle can have a dedicated power transfer coil and acquire the requisite power individually. The system operates at a near unity power factor with a small loss factor so the incremental operating costs of this technique are expected to be relatively small. The capital cost of the technique is on the order of $620/two-way meter, as detailed in Section 3. There are no significant guideway maintenance costs associated with this power transfer concept. The power transfer system is robust to individual switch failure since even several sequential failed switches can be tolerated.

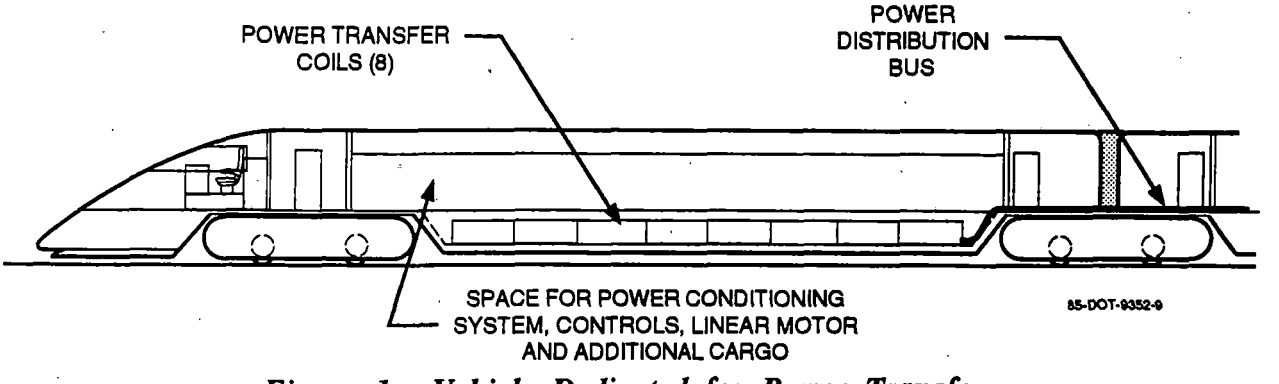

Figure 1. Vehicle Dedicated for Power Transfer

Issues with inductive power transfer include the following:

- Electromagnetic interference issues for:
  - Personnel
  - Equipment
- Waveform harmonic content
- Capital cost.

Additional analysis is required to resolve these issues. The electromagnetic interference question can be addressed by appropriate system and component design. The waveform harmonic content issue can be addressed by additional filter components. Experimental confirmation of this power transfer technique is required to validate the concept.

ES.6 Conclusions

In conclusion, we have examined several types of power transfer of the contact and non-contact types. We found significant shortcomings with existing power transfer implementations. The shortcomings manifested themselves as inadequacies in either high speed or high power transfer. The power transfer technique developed under this research shows great promise to efficiently transfer large amounts of power to vehicles of high and low speed in a non-contact, full air gap inductive manner.

An innovative application of a high frequency inductive technique is suggested for transfer of power at any speed. This technique was made practical by recent developments in high power semiconductor switches. Calculations show that a dc system can supply high power transferred by air core transformer action across the full air gap (100 mm) by the use of a resonant (tuned) circuit for on-board power factor correction. The total capital cost for this system is approximately $620/two-way meter.

ES.7 Recommendations

It is recommended that the non-contact inductive power transfer method proposed here be developed further by analytical and experimental investigation. Analytical studies are needed to further define and optimize the power transfer circuit characteristics especially for power levels above 10 MW. Experimental validation of the technique at the 100 kW level is recommended to verify that significant issues have been appropriately addressed.

1. INTRODUCTION

1.1 Background

Magnetically levitated transportation is being investigated as a method of transporting passengers and freight over relatively long distances (100 to 1,000 km) at relatively high speeds (135 m/s). Due to environmental and energy efficiency considerations the most viable Maglev options appear to be all-electric with the electric power being centrally generated, transmitted to the guideway and delivered to the vehicle. A typical high speed Maglev vehicle will require instantaneous power of 10 MW. This estimate is based upon an energy consumption of 980 J/passenger-km (1), and 75 passengers per vehicle. Several such vehicles traveling as a unit (a "train") will, of course, require additional power. Transporting 600 passengers in an eight vehicle train could require up to 40 MW of instantaneous power. This estimate uses the fact that at steady speed most of the energy consumption is due to air drag, and, of course, several vehicles in a train reduce the air drag per vehicle.

Maglev transportation could be driven, at least in part, by power transfer techniques. Proven electric power transfer techniques are typically limited to low powers and/or low speeds. Significant exceptions to this statement include the high speed rail enterprises French TGV (2) and German ICE (3) and prototype Maglev efforts Japanese Railway (MLU002) (4) and German Transrapid (TR07) (5). Under special circumstances, these high speed rail systems have demonstrated high power transfer (~10 MW) at high speed (135 m/s = 480 kph = 300 mph). The Maglev systems have transferred smaller levels of power (100-250 kW) at 135 m/s (300 mph).

If any of the power transfer techniques utilized in the above mentioned systems were wholly adequate, the power transfer problem could be considered solved, with remaining tasks being optimization of the existing techniques. Unfortunately, all previous power transfer techniques suffer from disadvantages (discussed later) which makes the development of a new power transfer technique desirable.

As part of this research, we reviewed a large volume of relevant literature on power transfer techniques. In addition to articles in English, we reviewed articles in Japanese, German and French. This literature is discussed and referenced throughout the report and listed in the bibliography.

The power required by a Maglev system serves two basic purposes: "drive" and "hotel" power requirements. Drive power is the power required to propel the vehicle at high speed. Depending upon the specific design and speed, power requirements can easily exceed 10 MW per vehicle to overcome aerodynamic drag and to provide hill climbing power. For this study we considered power requirements up to 40 MW, representing a multivehicle train.

When the instantaneous power requirement exceeds the power transferred, on-board power supplies, such as batteries, are used. These on-board supplies eventually must be recharged. Therefore, the hotel power transferred must be sufficient to restore the on-board supplies to ensure power availability in case of a service interruption.

1.2 Objectives

The objectives of this research were: firstly to determine the maximum practical power transferrable to a magnetically levitated (Maglev) vehicle traveling at high speed; and secondly, to develop a preliminary design of the optimum power transfer technique. We restricted our investigation of power transfer techniques to contact (brush) and non-contact (inductive) means.

In determining the optimum transfer technique, consideration was given to the following characteristics, among others: power regime, technical risk, safety of on-board or wayside personnel, electromagnetic interference, reliability, maintainability, vehicle weight impact, vehicle speed effects, sensitivity to traffic density, aerodynamic effects (drag and noise), esthetics, capital and operating costs, etc. A complete list of issues considered is given in the subsection 2.2.

1.3 Technology Issues

With regards to the actual transfer of power, the vehicle can be active and the guideway can be passive, or, conversely, the vehicle can be passive and the guideway can be active. The former situation is similar to present-day high speed electrified rail systems. In this case, the "guideway" is simply two well-aligned rails and the active vehicle propels itself down the track. Note that the existence of an intricate wayside high power delivery system delivering ~10 MW to the train does not disqualify the guideway from being identified as "passive."

The passive vehicle and active guideway system describes that chosen by both the Japanese and German maglev developers. In this case, drive power is delivered to motor coils embedded in

the surface of the guideway. The currents in the guideway directly interact with currents on the vehicle to propel the vehicle. Since the guideway delivers the drive power, the power to be transferred to the vehicle is greatly reduced. The vehicle need only receive hotel power to maintain operations.

Many studies have shown (19-21) that the guideway is the most expensive component of the entire system. To reduce the total system cost, anything which allows the use of a less expensive guideway should be investigated. The active vehicle concept holds the promise of a cheaper, passive guideway compared to the active guideway.

As a particular example of a passive guideway, a continuous sheet guideway has been proposed as an inexpensive option. The vehicle could then be propelled by linear induction motor (LIM) action and levitation and guidance provided either by on-board superconductors and/or on-board normal (resistive) magnets. In this case the full drive power must be transferred to the vehicle, conditioned appropriately and delivered to the electric motor. In essence, a tradeoff must be made between guideway cost and power transfer complexity.

High speed rail has made significant strides in developing high speed, high power transfer methods. In general, they rely upon contact means (brushes). For highest speeds and greatest powers, the rail systems typically use an overhead high voltage catenary wire and on-board pantograph for power collection. Unfortunately for power transfer, catenaries have unstable dynamic modes which are excited by high speed pantographs. On a test run, the French TGV has attained a speed of 143 m/s (9) while transferring approximately 8 MW via a 25 kV, 50 Hz single phase ac, single catenary, system. The current is returned through the rails. The track and overhead equipment were especially tuned for the record setting run. While representing a significant milestone for steel-wheel-on-rail systems, to achieve such performance for routine service would require constant, costly "tuning" of the system.

2. TECHNICAL ASSESSMENT OF CURRENT TECHNOLOGIES

2.1 Introduction

This section discusses the overall assessment of the concepts and technologies associated with the various power transfer systems.

2.2 Technology Assessment

An objective assessment of the technologies of power transfer is required to determine the optimum system. In order to perform this assessment, several alternative technologies were investigated and the concepts developed to some level of detail. In this subsection we describe the selection procedure developed by S. Pugh (22) and in the next subsection we present the results of evaluating eight different power transfer techniques.

2.2.1 Pugh's Selection Procedure

Pugh's selection procedure is a method of selecting concepts based on their ability to meet design objectives. Concepts are compared on a one to one basis utilizing a simple same as (S), better (+), or worse (-) comparison which provides a clear outcome based on ability to meet performance requirements. The approach not only provides a clear comparison of concepts; it also clarifies the performance requirements of the system and aids development of new improved concepts utilizing the best features of the concepts.

Several steps are required to perform Pugh's selection procedure. Each concept must be identified to a similar level of detail and must include key features and specifications. These concepts are arranged in a row at the top of a page (Table 1). Performance requirements are listed in a column along the left edge of the page. This process is very important since the performance requirements are not always well defined and may need some development effort. A concept is selected as the datum or baseline to serve as the basis of comparison. This is often an existing design for the first pass. The datum is compared with one other concept based on its ability to meet a performance requirement. The other concept is rated as being either the same, better, or worse than the datum at meeting the performance objective. Each concept is compared to the datum for its ability to meet that performance objective, and the process is repeated for each performance objective in turn.

Table 1. Comparison of Alternate Power Systems via Pugh Method

			Noncontact			Contact				
No.	Parameter		High Frequency Induction	Propulsion Harmonics	Super-Conductor Harmonics	Conventional Rigid Rail	Rolling Rigid Rail	ac Catenary	dc Catenary	Side Grabber Catenary
1	Hotel Power		Baseline	S	S	S	S	S	S	S
2*	Drive Power		Baseline	-	-	S	S	S	S	S
3	Speed Dependency		Baseline	-	-	-	-	-	-	-
4*	Safety		Baseline	S	S	-	-	-	-	-
5	Electromagnetic Interference		Baseline	S	S	-	-	-	-	-
6	Degradation Sensitivity		Baseline	S	S	S	S	S	S	S
7	Traffic Density Sensitivity		Baseline	-	-	S	S	S	S	S
8	Hotel Power Proven?		Baseline	+	+	+	+	+	S	-
9	Drive Power Prven?		Baseline	-	-	-	+	+	S	-
10	Speed Proven?		Baseline	+	+	+	+	+	-	-
11	Drive Power and Speed Proven?		Baseline	-	-	-	+	+	-	-
12*	Reliability		Baseline	S	S	-	-	-	-	-
13*	Maintainable?		Baseline	S	S	-	-	-	-	-
14*	Acoustic Noise		Baseline	S	S	-	-	-	-	-
15*	Aerodynamic Drag		Baseline	S	S	-	-	-	-	-
16*	Esthetics		Baseline	S	S	-	-	-	-	-
17	Effect on Utilities		Baseline	S	S	-	-	-	S	-
18*	Capital Cost		Baseline	+	+	+	+	+	+	+
19*	Operating Cost		Baseline	-	-	-	-	-	-	-
	Totals:	+		4	4	4	5	5	2	1
		S		10	10	4	5	4	6	4
		-		5	5	11	9	10	11	14
*	Totals of high priority parameters:	+		1	1	1	1	1	1	1
		S		6	6	1	1	1	1	1
		-		2	2	7	7	7	7	7

* Marks a high priority parameter.
S, +, -: Same, better or worse than baseline, respectively.

It is important to maintain the same interpretation of the performance objective for each comparison, thus, the comparisons are made one row at a time. The concepts must not be changed as the process proceeds since that could change the results of decisions that were made previously about a different performance objective. Instead, a new concept is created incorporating the desired changes. The new concept is set aside until all of the performance requirement comparisons have been completed. The result of the process is a chart which contains a clear evaluation of the strengths and weaknesses of the concepts in their ability to meet the design requirements relative to the datum.

Usually, in addition to the chart, there are a few new or refined concepts that became apparent during the evaluation as well as some new or clarified performance requirements that need to be included. Some of the concepts can be discarded based on deficiencies in a key performance requirement. At this point the comparison process is repeated incorporating the new concepts and requirements. Since all comparisons are relative to the datum, there is no information on the relative merits of each concept, that is which concept that was better than the datum is better than the others. For this reason it is often desirable to select another promising concept as the datum and do another chart to clarify differences between promising concepts. By repeating the entire process for the promising concepts, the strengths and weaknesses of the concepts become apparent.

The number of better (+) and worse (-) scores can be tallied to provide a rough ranking of the designs; however, since some performance requirements are more important than others, it is better to investigate which concepts best meet the most important requirements. Pugh's process results in a chart which provides a quick reference to the strengths and weaknesses of concepts relative to a baseline design. The process usually requires a few iterations as the concepts are refined. The process of defining the performance requirements is critical to the success of the project. Sometimes the best choice is not the concept with the highest overall score, but the one that is best at the most important performance requirements. Thus, the result is not determined from a numerical score; it is determined primarily from a tradeoff of what are considered to be the most important performance criteria.

Strengths of Pugh's process are:

- Comparisons are based on a one on one contest which is the most accurate and simplest way to compare things

- The simple three level scheme of same, better, or worse is less prone to bias and more consistent than numerical ranking schemes

- Performance requirements are clearly listed and are the basis of evaluation

- A record is maintained of the disadvantages as well as the advantages of the concepts

- Final selection is based primarily on selection of the most important performance requirements, which is in itself a key choice which must be made and documented

- Pugh's process reduces the effect of pre-existing biases and is relatively easy to check.

Pugh's process does not:

- Result in a numerical score that automatically selects a concept based on some composite sample of requirements

- Rely on a fuzzy grading scale that allows unconscious or conscious biases to add up and produce a large effect

- Eliminate the need to think carefully about what the important factors are.

The simple ranking scheme is good for reducing the bias of a particular individual and this is frequently one of the key strong points relative to many other approaches. Pugh's process has proven itself to be an excellent way to develop and select concepts in actual practice, and has frequently served to aid in a design decision by clarifying the ramifications of a design or system decision that had previously bogged down a project.

2.2.2 Results of Pugh Selection Procedure

The result of applying Pugh's selection procedure to the power transfer concepts is presented in Table 1. The first three columns are non-contact methods: the recommended high frequency inductive method, propulsion harmonics and superconductor harmonics. The next five columns are rigid rail (conventional and rolling brush) and catenary (ac line, dc line and side grabber, discussed below) methods.

2.3 Contact Means

2.3.1 Conventional Catenary/Pantograph

Conventional catenary and pantograph systems consist of overhead electrical equipment whereby a stationary block energized wire is contacted by an on-board pantograph. Various catenary designs are shown in Figure 2. Catenaries have been used successfully in the French TGV, German ICE and Japanese Shinkansen high speed rail systems. The TGV, ICE, and Shinkansen systems have demonstrated top speeds of 482 kph (300 mph), 407 kph (254 mph), 319 kph (200 mph), respectively (23). Figure 3 shows the principal electrical circuit used for TGV. Figure 4 shows a propulsion system similar to that used for ICE (24).

Although simple in concept, at high speed the pantograph excites transverse vibrational modes in the flexible catenary. High power transfer from a catenary is a system problem at any speed. A high voltage, continuously exposed wire means a potential safety issue with personnel and foreign objects. Other issues with a catenary include: aerodynamic effects, especially noise and tunnel entrance and exit; contact wire and pantograph wear; and poor esthetics associated with overhead equipment.

The system operating parameters establish fundamental power transfer limits. The catenary can be energized by direct current or single phase alternating current, although alternating current is used uniformly by the above mentioned systems. The voltage levels and excitation frequencies for high speed rail vary from 15 kV, 16 2/3 Hz for the ICE to 25 kV, 50 Hz for TGV (60 Hz for the

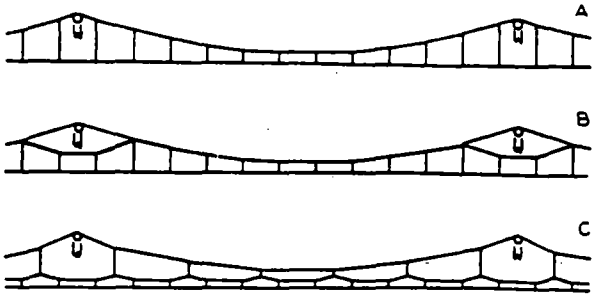

Figure 2. Common Forms of Catenary Systems. A, Simple Catenary; B, Stitched Catenary, C, Compound Catenary

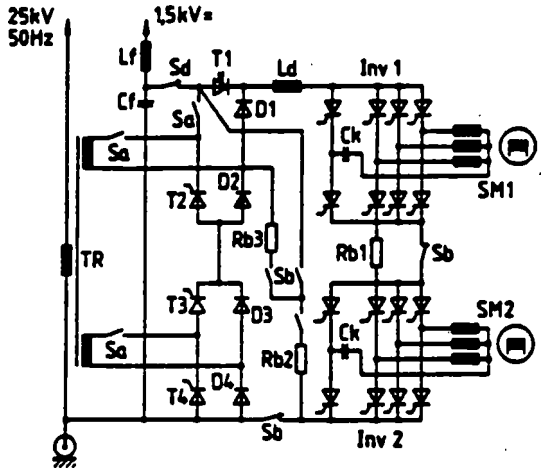

Figure 3. TGV Drive Circuit

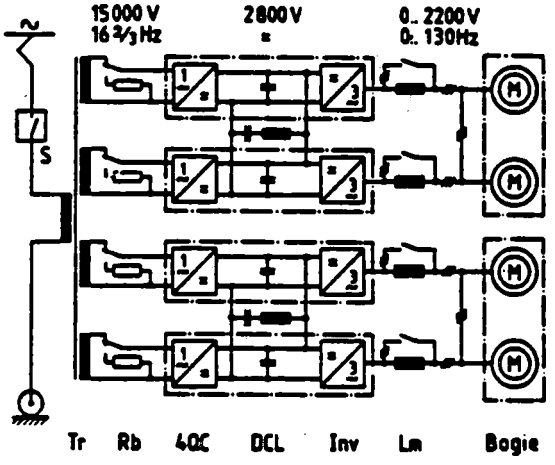

Figure 4. ICE-Like Drive Circuit

Texas TGV). In the United States, lower speed electrified rail systems have voltage levels up to 50 kV (25). The maximum current per pantograph is an important system parameter. A typical maximum current draw is 670A per pantograph (26,27).

The question of number of pantographs on a given catenary is answered by assessing the high speed catenary dynamics. The TGV uses a single pantograph due to the catenary dynamics excited by the passage of a pantograph.(28,29) Recall the current is returned through the rails. Other

investigators have found that the maximum train speed before loss of contact between wire and pantograph becomes significant is lower for two pantographs (one trailing) than for a single pantograph (30). Similarly, the Series 300 Shinkansen is reducing the number of pantographs to two, although part of the motivation for this was aerodynamic noise reduction.(31).

It is of interest to calculate the maximum transferred power in single phase and three phase catenary services. For these calculations we assume a maximum supply voltage V = 25 kVrms and a maximum current collection I = 670 Arms.

Single phase systems are relatively straightforward. The power is the product of the rms voltage and rms current: P = V I = 17 MW. Based on this fundamental result, there is significant technical risk for a single phase catenary/pantograph system attaining 40 MW of transferred power.

We consider three different three phase systems: the first system is similar to that proven by research conducted in the 1970s in the TACRV system (13, 44), the second system is an extrapolation of the proven system by increasing the supply voltage by a factor of 3, the third system is an extrapolation of the first system by increasing the supply voltage by a factor of 3 and the current collection by 40%. It is important to note that the second and third systems are hypothetical and represent increasing levels of technical risk. The proven system had a supply voltage of V_1=8250 Vrms and I_1=485 Arms which resulted in a power of 12 MW (13,44). For the second system (V_2=25 kVrms, I_2=485 Arms) we have a power capability of 36 MW. For the third system (V_3=25 kVrms, I_3=670 Arms) we have an available power of 50 MW. A three phase catenary system could be designed as three parallel overhead lines. However, due to the requirements for electric isolation in air, the total span of the lines would exceed 5 meters. An alternative would be to have one phase physically overhead, and one phase each on the port and starboard sides of the vehicle. In any event, incorporating a three phase catenary system would entail technical risk associated with location of the lines and pantograph operation on them. In summary, three phase catenary systems in principle can transfer the required power, but there is substantial technical risk associated with these hypothetical systems. In addition, the reliability and maintainability of these systems are unknown and they are likely to have very poor aesthetics.

To increase current collection it has been suggested (32) that a second pantograph on a single catenary could follow the first if approximately 200 meters separated them, but there is no experimental evidence substantiating this claim. Hence, in all cases, there is substantial technical risk associated with extending the power regime to 40 MW for catenaries and pantographs.

The design and development of catenaries and pantographs for high speed power transfer is a demanding task which must be approached from a system viewpoint. Nevertheless, for convenience, catenaries and pantographs are discussed sequentially.

At low speeds, catenary dynamics are well predicted by relatively simple models of the interaction of the pantograph and catenary (33). At increased train speeds, it is a well established experimental fact that increasing the tension of the contact wire maintains a dynamically stable catenary (34). This is readily explained as follows: The contact force of the pantograph excites a transverse traveling wave within the contact wire. The speed of this wave is equal to the square root of the ratio of wire tension divided by the wire mass per unit length. ... The important parameter for catenary dynamic stability is the ratio, r=v/c, of the vehicle speed, v, and the wave speed, c=sqrt(T/ρA), where T is the wire tension, ρ is the mass density of the wire material and A is the wire cross-sectional area. For r <<1 the catenary is stable. Typical numerical parameters for a high speed catenary (Texas TGV) are: catenary tension=20 kN, wire mass per unit length = 1.3 kg/m, and v=85 m/s (190 mph) [ref.: Andre Huber, GEC Alsthom, private communication, 10 October 1991.] so c=123 m/s and r=0.7. It is desired to have r approximately constant to retain stable dynamic catenary characteristics. Increases in maximum vehicle speed must be compensated by corresponding increases in wire tension, otherwise, as the vehicle speed increases, r will increase. As r approaches a value of unity, various modes or resonances of the catenary are excited causing significant deformation of the catenary shape [ref.: Tsuchiya, K. "The Dynamic Behavior of Overhead Catenary Wire Systems," Quarterly Report of RTRI, Vol. 10, No. 4, Dec. 1969, p. 251]. High amplitude dynamic deformations cause loss of contact between pantograph and catenary, interrupting the transfer of power to the vehicle, and excessive catenary wire wear (41).

Another detrimental effect of the catenary is electromagnetic interference of nearby electrical equipment (35). In the case of TGV, interference between the rail supply line and the telephone system was experienced to such an extent that maps of the networks were made to determine optmium placement of electrical equipment to *minimize* (not eliminate) the effects. Necessary additional protective countermeasures were decided jointly between the telephone and railway companies and *paid for by the railway* (emphasis added).

The design and development of high speed pantographs is a trade-off among the areas of electrical, mechanical, structural and aerodynamic performance. Current-carrying performance increases with increasing contact force while the amplitude of the catenary oscillations increase with increased contact force making it difficult for the pantograph servomotor to follow. In

addition, as vehicle speeds increase, the limited bandwidth of the pantograph mechanism must be considered. To reduce the disturbance to the overhead equipment the pantograph dynamic mechanical impedance and the contact force both should be as low as possible.

The probability of loss of contact between the contact wire and the pantograph $P_L(v)$ increases markedly with increasing speed (36). The reference documents the result of $P_L(500 \text{ kph}) = 20$ percent for the system investigated. The loss of contact means a substantially greater voltage drop between the wire and pantograph, and results in the formulation of an electric arc.

The pantograph mechanical impedance is the classic 'minimum un-sprung mass' problem. One would like to make the pantograph as light as possible (37). Unfortunately, the pantograph must have structural strength to handle the severe loads imposed by the contact force, the dynamic motion of the pantograph itself and aerodynamic forces.

Aerodynamic forces are sufficiently great to have been the cause of several high speed "incidents" on the TGV (38). It was found that in the presence of a strong cross-wind, enough lift was generated on the pantograph to cause it to hit the registration arm supporting the contact wire which damaged many kilometers of the overhead catenary system. On the Shinkansen, the aerodynamically generated noise of the pantographs is significant and one of the reasons for reducing the number of pantographs (39). The German Federal Railway experience is that the entrance/exit to tunnels subjected the pantograph arm to vibrations which caused extreme aerodynamic-induced bending loads (40).

Wear of the contact wire and the pantograph contact strip (usually graphite) in high speed operations of electric trains is one of the most important problems in maintenance concerning current collection (41). The life of a contact wire is determined not by the average wear of the total wire but by certain points on the wire experiencing the greatest wear.

Two important factors determining wire wear are the mechanical contact force and electrical erosion caused by arcing. Impulsive contact forces are often experienced at the wire overlap of a connecting section of the contact wire. Detailed analysis of the contact force shows that fluctuation of contact force is correlated with wear of the wire (41). A Fourier analysis of the fluctuating current waveform identified specific natural frequencies associated with current collection and these frequencies were identified with different bending modes of the pantograph. These mechanical vibrations at the pantograph natural frequency can have a sufficient amplitude to cause loss of

contact and arcing. The combination of alternating impulsive loads and arcing due to loss of contact is the most severe condition for wear of the contact wire (41).

The present-day cost of a catenary system can be estimated from analyses made ten years ago (42). In the referenced study the one way cost was $200k/mile (1981 dollars). Using an inflation factor of 5 percent pa, we would expect a similar system to cost approximately $340k/mile today.

2.3.2 Enclosed Horizontal Catenary

A design for an enclosed catenary is shown in Figure 5. This design alleviates some, but not all, of the shortcomings of catenary systems. Some of the advantages of this system are reduced acoustic noise, better catenary dynamics, and better esthetics. The noise problem is less, and the esthetics better, because of the enclosed nature of the structure. The catenary dynamics are improved since the catenary can be held at a lesser span interval, making the system stiffer. Unfortunately, this system does not solve the fundamental problem of electrical loss of contact.

2.3.3 Catenary Side Grabber

A design which improves the electrical current collection characteristics of a catenary system is shown in Figure 6. In this design, the catenary is held by sliding or rolling brushes from opposing sides. Therefore, the contact force can be quite high but the transverse force, which excites the catenary dynamics, can be nearly zero. This design has advantages of better catenary dynamics and improved electrical contact, but suffers from increased mechanical complexity. Of course, the design described here can be combined with that described in the previous subsection.

A key problem with catenary based power transfer at high speeds is dynamic behavior of the catenary excited by the moving brush contact force. The majority of the catenary excitation is produced by the force normal to the catenary surface, with the drag component producing a minor effect. Contact force adequate to provide good contact for power transfer excites the catenary dynamically. The catenary side grabber illustrated in Figure 6 provides the necessary contact force by pinching the conductor wire between two contoured brushes. This allows any desired contact force to be maintained for electrical contact with no net force perpendicular to the wire. Catenary tracking is then decoupled from the problem of catenary-brush contact pressure. The approach shown in the figure utilizes a force and torque sensor to provide a feedback signal to the pickup arm position controller. The controller responds to the lateral or vertical forces measured to track the catenary and keep the lateral forces on the conductor to a minimum. The brushes are spring

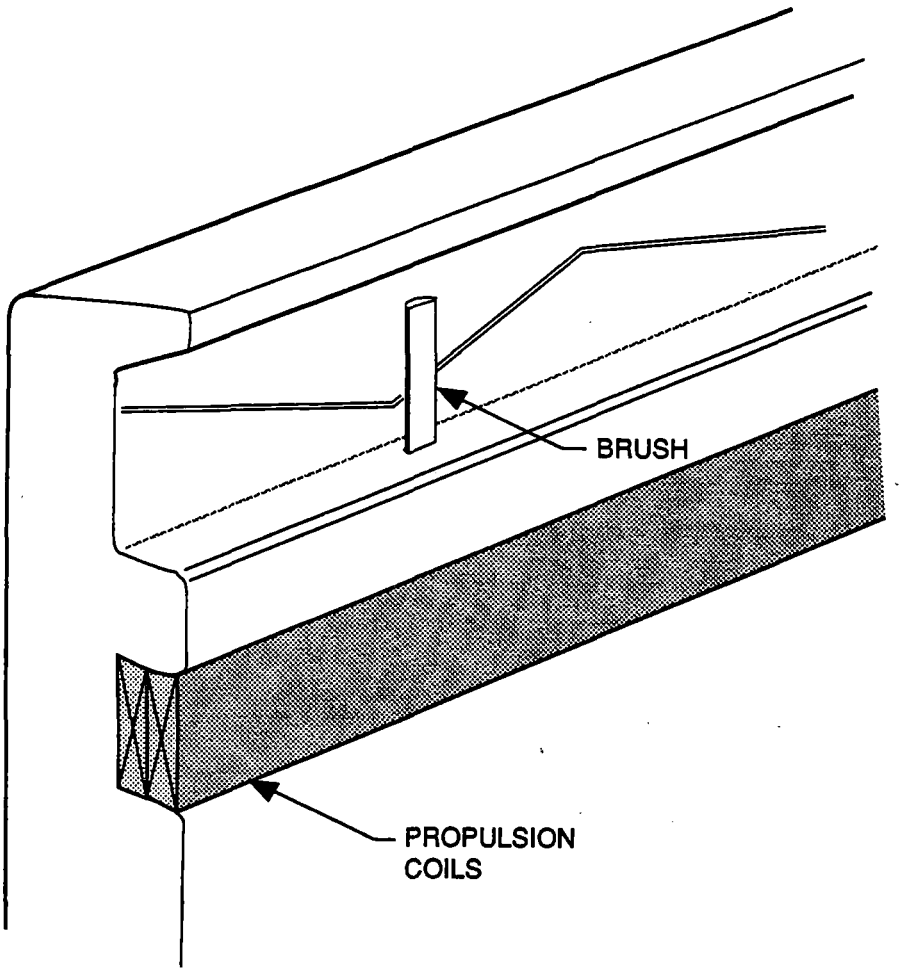

Figure 5. Enclosed Horizontal Catenary

loaded and designed to accommodate wear and be replaced easily. The spring also allows the brushes to accommodate variations in catenary size and any small rapid motion required above the response capability of the positioning system. Figure 6 is a representative schematic; other methods of tracking the motion of the conductor could be used. Multiple redundant brushes can be utilized since excitation of the catenary is reduced. The brushes can be snapped onto the catenary by a vertical motion of the position controller. Leading and trailing edges of the brushes would be bevelled to aid catenary tracking. It may be possible to design a very light and reliable system that reduces or eliminates the requirements of the brush positioning system.

Catenary sag due to thermal expansion produces significant variations in the shape of the catenary. A material with a negative coefficient of thermal expansion, or thermomechanical

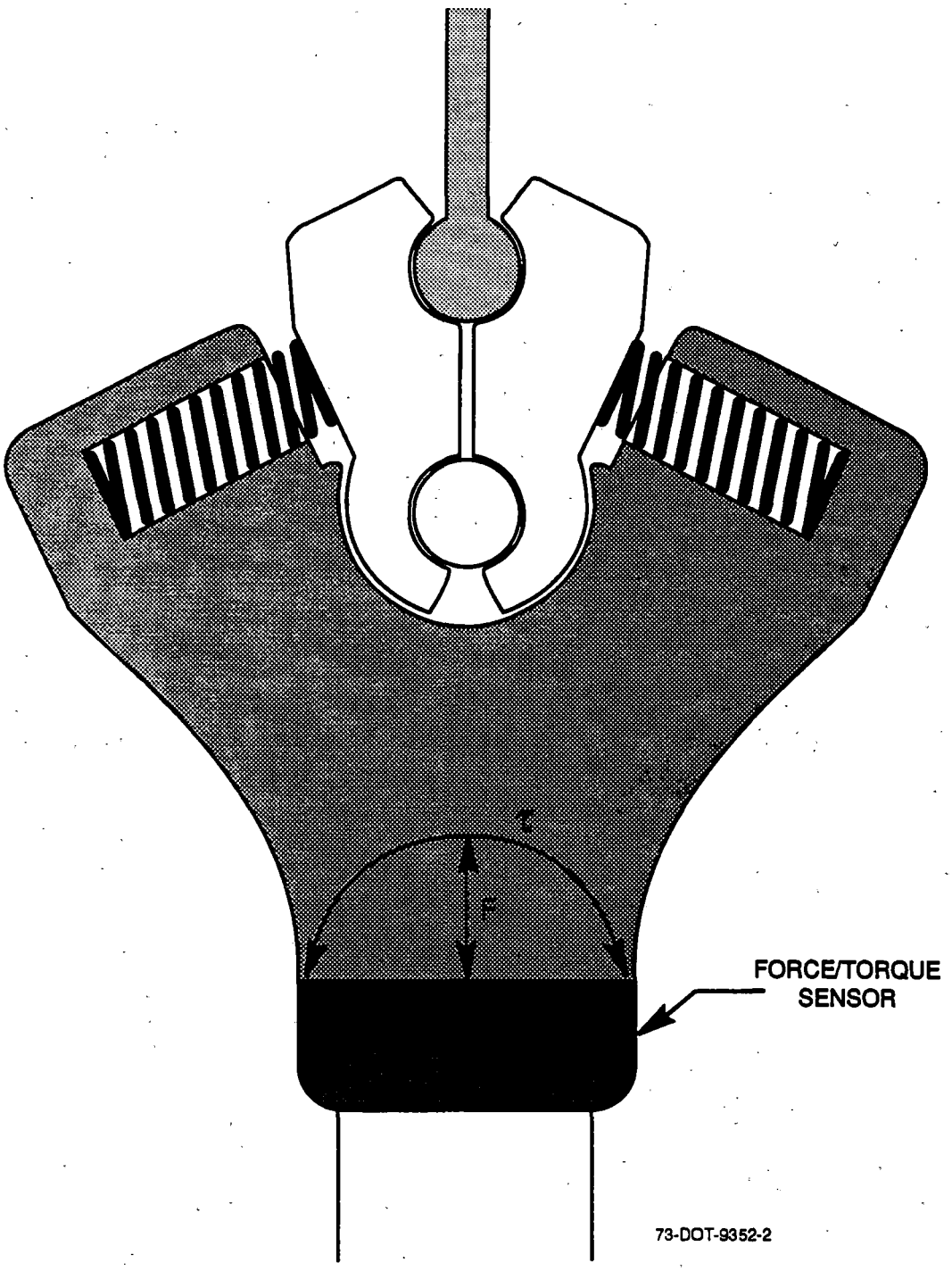

Figure 6. Catenary Side Grabber

actuators utilizing phase change materials, bimetals, etc., could be utilized to reduce variation in the shape of the catenary due to temperature variations.

2.3.4 Rigid Rail/Brush

Catenaries and rigid rails are the two common contact means of power transfer. Rigid rail (often called "third rail" when there are two rails used for guidance) is typically thought of for lower speeds and lower voltages than catenaries. Nevertheless, there has been significant research (43-47), although some of it is dated, which presents rigid rail power transfer as a viable approach. (Here we exclude from consideration reproduction of the conditions under which the catenary system returns current through the rails since it requires impractically large contact forces.)

2.3.4.1 Conventional Rigid Rail/Sliding Brush

Perhaps the most well-developed sliding brush power transfer concept is the one used for the Tracked Air Cushion Research Vehicle (TACRV). The design was for three phase, 60 Hz current collection at 135 m/s with carbon brushes using two brush sets. The design power was 12 MW at 8.25 kV and 485A through 12 brushes per phase (48). This concept was tested at high speed on a rocket sled to 313 mph with a circulating current of 1000A. Figure 7 shows the delta configuration of the brushes. Unfortunately, this system was never demonstrated with an inductive load. This three phase system had an advantage over single phase due to the balanced three-phase operation. This alleviates the unbalanced load conditions which exist at the substation with single phase systems.

The disadvantages of this system are the increased expense compared to a catenary and the high brush wear, and hence, high maintenance typical of sliding brushes.

2.3.4.2 Rolling Brushes

Rolling brushes are desirable because of the reduced speed of the contact point. A system has been demonstrated which appears to offer promise for the high speed, high power requirements of this program (49). (See Figure 8.) The reference documents a current collection system operating at 500A, 120 m/s = 270 mph, with a projected brush life of 7,000 km. The system was designed for a peak power transfer of 17 MW.

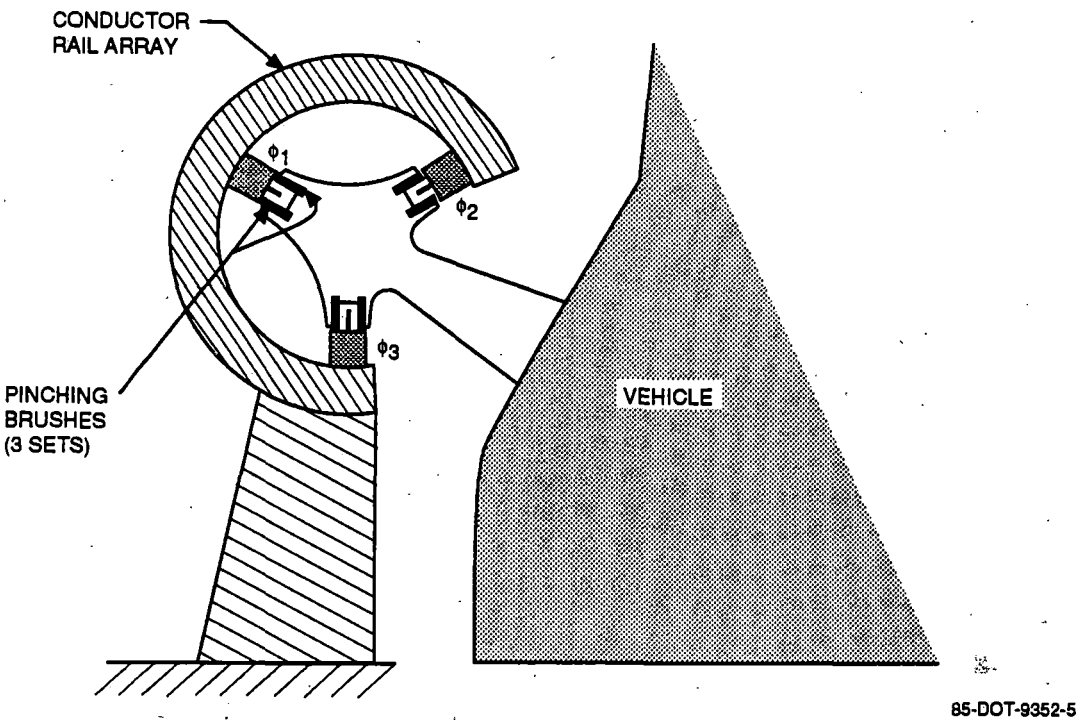

Figure 7. Rigid Rail Power Transfer

Although this work is encouraging, the experimental set-up differed in an important manner from true field conditions. The experiment described in the reference was for current collection between a rotating brush and a rotating slip-ring representing the stationary power rail. In the experiment the slipring would tend to become "polished" and de-burred by the rotating brushes, hence becoming an ever-smoother slip-ring. On the other hand, in the field, the brushes would continuously encounter virgin rail. Environmental corrosive effects would be expected to continuously roughen the rail surface. The rougher rail might lead to a greater brush wear rate.

The Japanese attempted to use rolling brushes for low speed power transfer (50). They used a copper braid or mesh on the periphery of the levitation wheel. Measurements reported in the reference indicate that the tire surface heated with increases in current, the dissipative losses increase linearly with current because the voltage drop was constant (0.6V), and the tire temperature increased with rolling speed at constant current. Currents up to 300A were tested, and maximum velocities were 30 m/s. It was noted that the acoustic noise from the copper braided tire was actually less than that from an ordinary car tire.

ROTATING WIRE BRUSH ASSEMBLY AND SYSTEM

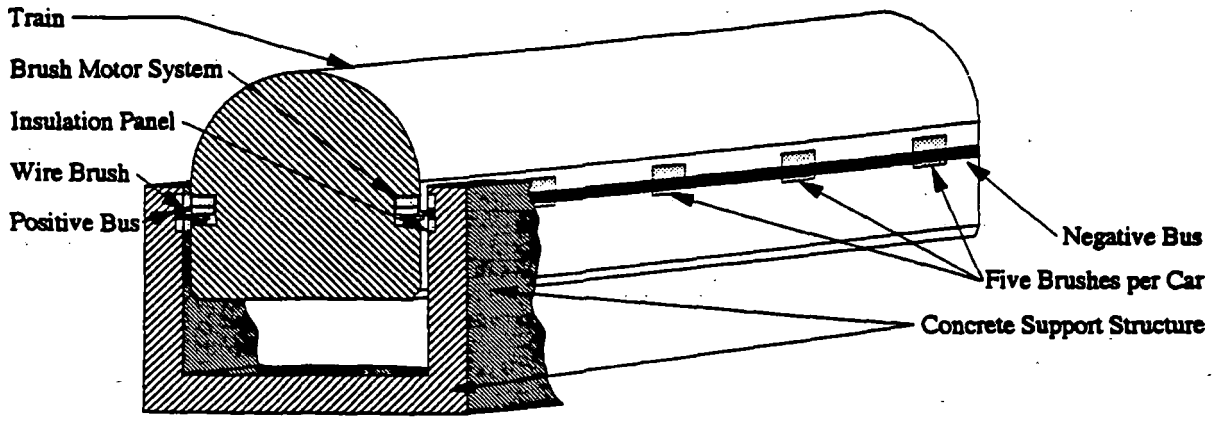

Train Cross Section and Side View

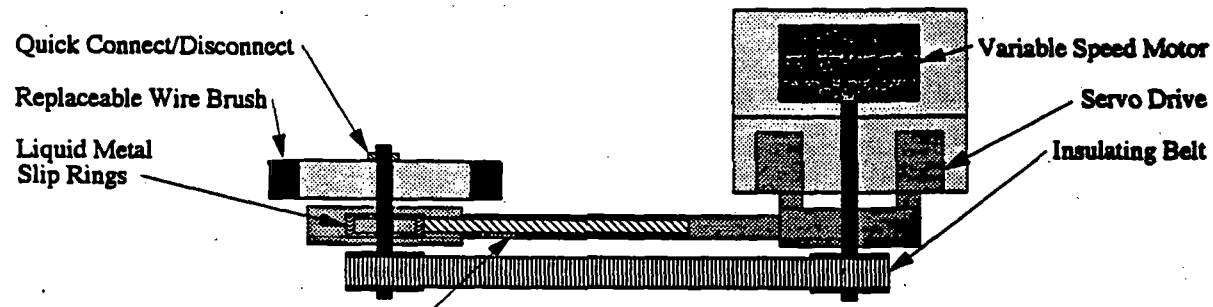

Wire Brush Side View

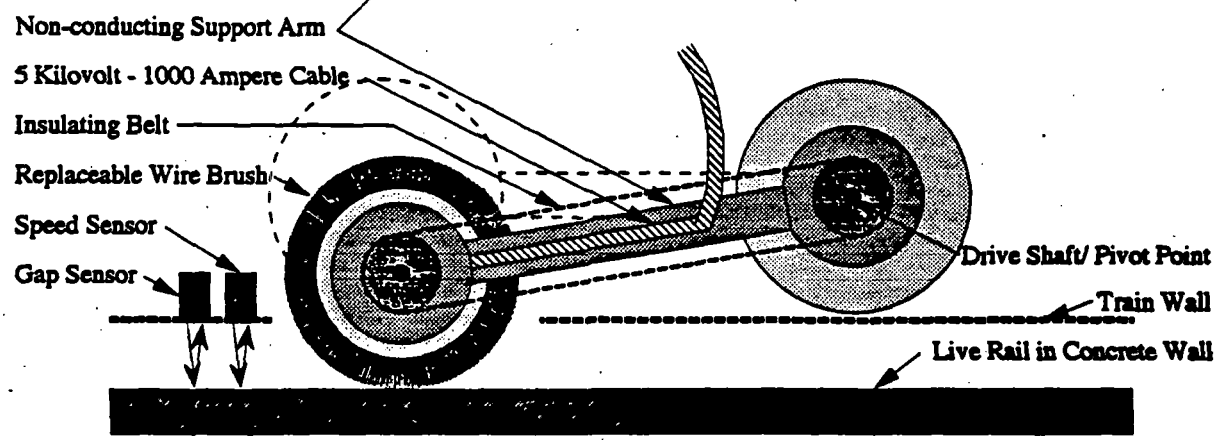

Wire Brush Bottom View

Figure 8. Rolling Stock Power Transfer

2.4 Non-Contact Means

We considered two types of non-contact power transfer means: parasitic and dedicated power collection. The parasitic power transfer means includes induced harmonics of the superconducting coil as it passes the levitation coils and induced harmonics of the propulsion coils as the vehicle passes them. In both cases the power is collected on-board the vehicle by pick-up coils. The dedicated power collection coil system described in the next section consists of relatively large wayside and vehicular facing coils. The power is derived from an ac or locally inverted dc bus.

2.4.1 Harmonic Pick-up

The power collected by this technique is parasitic power in nature which implies it is always a small fraction of the fundamental power. In addition, the power is inefficiently transferred and it increases the magnetic drag, i.e., it increases the required propulsive force. (See Figure 9.)

2.4.1.1 Superconductor-induced Harmonics

This method is described in detail in the reference (17). This method relies upon large circulating currents in the levitation coils which, from the frame of reference of the train, appear to pulsate. As demonstrated experimentally, this method has been used to the 100 kW level with horizontal ground coils. Unfortunately, the power transferred is dependent upon the square of the vehicle speed. At vehicle speeds below 111 m/s a supplemental power source such as on-board batteries is required. At standstill in the station, power is transferred to the vehicle via contactors

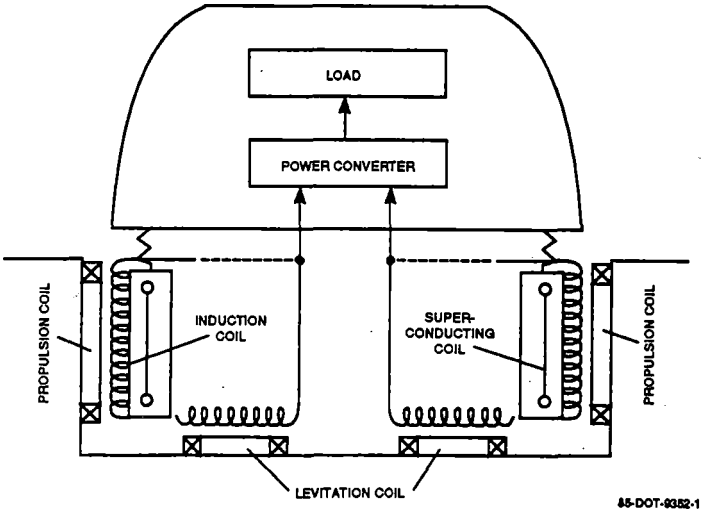

Figure 9. Harmonic Power Transfer

(stationary brushes). The batteries are charged inductively when speeds exceed 111 m/s or by brush power transfer when the vehicle is in the station.

Maximizing this power transfer technique implies making greater the power content of the spatial harmonics of the levitation coils which in turn produce temporal variations of the flux through the induction coil. Variation in this pulsating flux, by definition, increases the variability of the local levitation force. In principle, on-board coils can be averaged to produce a smoothed levitation force. In addition, secondary suspension systems could be designed to accommodate these variations in levitation.

This method suffers from a poor power transfer efficiency even at the highest speeds and poor power transfer capability at low or medium speeds. As an example of transfer efficiency, to transfer 50 kW to the vehicle, approximately 225 kW (40 percent efficient) must be transferred to the guideway wayside. This amounts to several percent of the total drive power of the vehicle.

The power transferred is limited to a fraction of the levitation and propulsion power and thus certainly cannot be used for transfer of propulsive power. This technique appears to work satisfactorily for transfer of hotel power to high speed vehicles.

2.4.1.2 Propulsion Coil-Induced Harmonics

This method relies upon the spatial harmonics of the propulsion coils as seen from the frame of reference of the vehicle. Because the current-turns product for propulsion is an order of magnitude less than for levitation, the power transferred is so much less that even at high speed only minimal hotel power can be transferred (7kW) (17). In addition, the propulsion power is generally designed to provide smooth propulsion forces. An example of this is the introduction of three electrical phase, two-layer propulsion coils by the Japan Railway organization.

Increasing the magnetic coupling by the introduction of iron flux paths can dramatically increase the effectiveness of the harmonics associated with the propulsion currents. This technique has been demonstrated on the Transrapid Maglev system (5). (See Figure 10.). The power transferred is linearly proportional to vehicle speed.

In this system approximately 250 kW is transferred to the vehicle by harmonic magnetic flux of the propulsion currents at speeds greater than 35 m/s. Below this speed on-board batteries

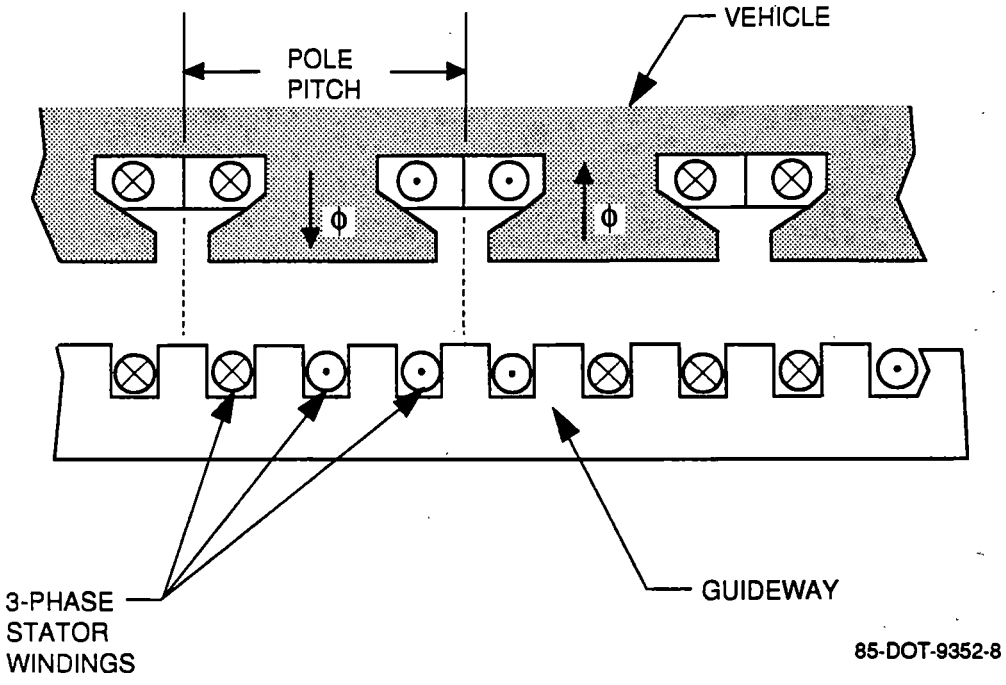

Figure 10. Inductive Ferromagnetic Core Variable Frequency Power Transfer

supply the needed power. This system requires substantial ferromagnetic mass to provide the improved magnetic coupling. The effect of the ferromagnetic mass depends upon the application. In some applications, such as train rolling stock, adding mass to accomplish power transfer may be acceptable. Attractive magnetic levitation systems which already have ferromagnetic mass for another purpose can use this mass in transferring power. Essentially, the ferromagnetic mass is already present and no additional mass is required for power transfer. In other applications, however, the added mass is a serious detriment to system performance. This is particularly true for large gap magnetic levitation systems which rely on superconductive magnets to provide the lift force. The power transfer efficiency is approximately 80 to 90 percent.

3. RECOMMENDED POWER TRANSFER TECHNIQUE: HIGH FREQUENCY DEDICATED COILS

A single phase high frequency dedicated coil system is the power transfer technique recommended by this report. In this approach, power is transferred by air core transformer action between the stationary guideway and the moving vehicle across the full air gap. Power coupling is greatly improved over the parasitic methods in four key ways:

- The mutual inductance can be made large without massive ferromagnetic material by optimized coil geometry.

- The frequency of excitation can be high, hence, for a given number of ampere-turns the transformed voltage can be large.

- An on-board resonant circuit can be used to tune out reactive components of power. The impedance of the power transfer coil is purely resistive as seen from the viewpoint of the wayside power source.

- Power transfer can be accomplished at all speeds, including standstill.

To improve the efficiency the coils are large compared to the gap. This also produces an increase in power transfer capability.

In this section, we will first describe a 1 MW inductively coupled hotel power transfer system which can be built with current state-of-the-art solid state components. We will show that in principle 40 MW can also be transferred. Figure 11 shows a simplified electrical schematic of the guideway system. Initially, 480 Vac, 60 Hz utility power is rectified to produce about 500 Vdc. A full bridge Insulated Gate Bipolar Transistor (IGBT) inverter chops the dc into 1 kHz square wave which then is stepped up to about 2,700 Vrms by a laminated steel core transformer. The 1 MW inverter and step-up transformer would be about 2 m^3 in size and cost on the order of $50,000. The 1 kHz single phase guideway bus will carry about 600 Amperes and could have an inductance per unit length, L', as low as L' = 0.3 μH/m. With inverters every 1.6 km, the bus inductive voltage drop would be on the order of

$$V_L = L\, dI/dt = 800m * 0.3 \times 10^{-6}\ H * 2\pi * 1000\ Hz * 600A = 900V$$

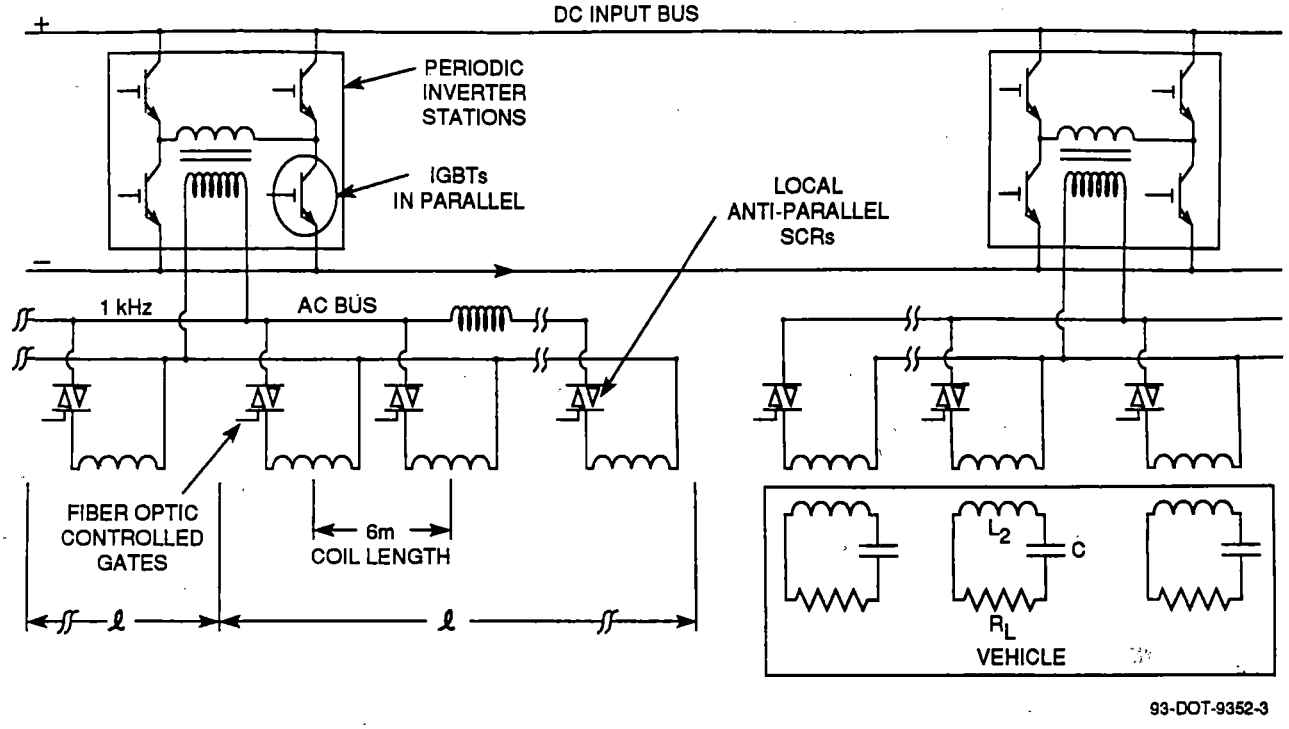

Figure 11. High Frequency Power Transfer Electrical Schematic

This voltage drop is reactive and can be compensated by power factor correction at the inverter station if necessary.

The guideway coils will be approximately 1.6m high and 6m along the guideway. The coils will be wound with 45 turns of No.10 gauge copper wire for an inductance of 29 mH and a resistance of about 2Ω.

Considering the case of a multi-vehicle train, we assume 10 vehicles and 100 kW/vehicle hotel power. Each vehicle spans three coils and the current per coil is approximately 20A which corresponds to a 40V resistive drop per coil. This is small compared to the bus voltage. Unlike the reactive bus voltage drop, however, the coil losses are not recoverable. The guideway coils can be switched locally to the 1 kHz bus by a pair of anti-parallel high voltage silicon controlled rectifiers (SCRs) as the vehicle passes each coil. The onboard pick-up coil is 18m in length and 1.6m high. Thus, it overlaps between three and four guideway coils. The guideway coils are switched sequentially along the guideway to maximize the effective coupling. A key feature of the proposed power transfer technique is that the secondary coil system on the vehicle is a tuned LRC

circuit. The tuned circuit effectively compensates for the imperfect air core coupling between the guideway and vehicle coils due to the finite air gap.

Figure 12 shows an electrical schematic for the power transfer circuit. The air core transformer is modeled as a four port device described by two linear differential equations. The self and mutual inductances are L and M, respectively. The coil resistances are relatively small and are neglected in this simplified analysis. The transformer can be modeled as a Π section, as shown in Figure 13, or "T" section, as shown in Figure 14. For convenience, we assume the primary and secondary self inductances, L_1 and L_2, are such that $L_1 = L_2 = L = 29$ mH and that the mutual inductance $M = 14$ mH.

As seen from the output of the transformer, the combination of the voltage source and "T" model can be further modeled as a Thevenin voltage source and Thevenin series impedance (Figure 15). The Thevenin voltage, V_T, can be found by examining the inductive voltage divider composed of inductances (L-M) and M and is

$$V_T = V_0 * k$$

where $k = M/L$ is the coupling constant of the air core transformer. With an air gap of 10 cm the coupling constant is approximately 0.5 with coils facing each other. The reduction in coupling due to translation along the guideway is less than 20 percent.

The Thevenin impedance, $j\omega L_T$, is found by short circuiting the source and calculating the output impedance of the "T" section, where

$$L_T = L\,(1-k^2)$$

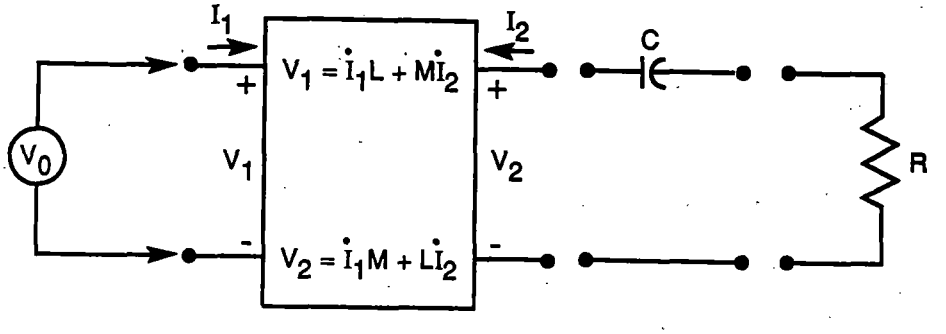

Figure 12. Power Transfer Electrical Circuit

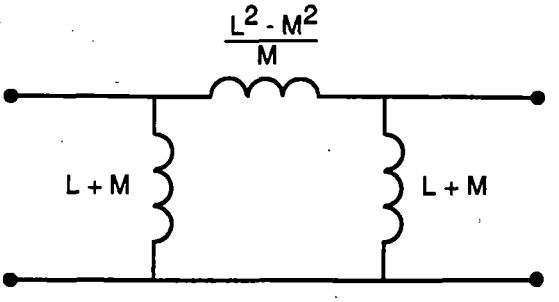

Figure 13. Transformer "Π" Section

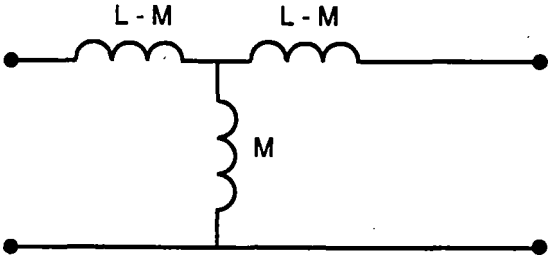

Figure 14. Transformer "T" Section

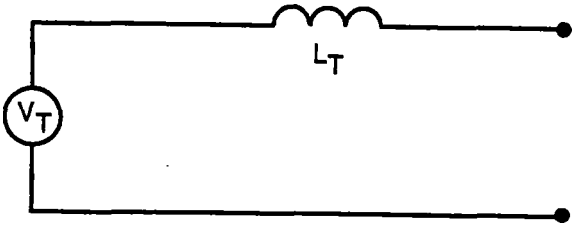

92-DOT-9352-3

Figure 15. Thevenin Equivalent Circuit

The series inductive reactance, X_T, can be exactly cancelled by a series capacitive reactance, X_C, as shown in Figure 16, at a frequency equal to

$$\omega_0 = \frac{1}{\sqrt{L_T C}} = \frac{1}{\sqrt{LC(1-k^2)}}.$$

The resulting circuit is shown in Figure 17 where the Thevenin voltage source is directly connected to the load. Note that V_T is reduced from V_0 by the coupling constant, k. The power delivered to the load is

$$P = V_T^2/R = V_0^2 k^2/R$$

and thus the effective load impedance as seen from the source is the actual impedance multiplied by a factor of $1/k^2$. This power is rectified and conditioned on-board the vehicle for usage at about 1,800V and 60A (as shown in Figure 18).

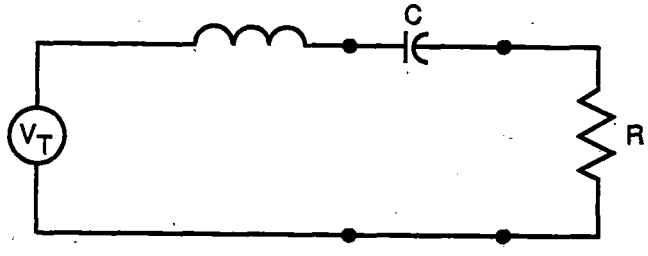

85-DOT-9352-7A

Figure 16. Thevenin Series Circuit

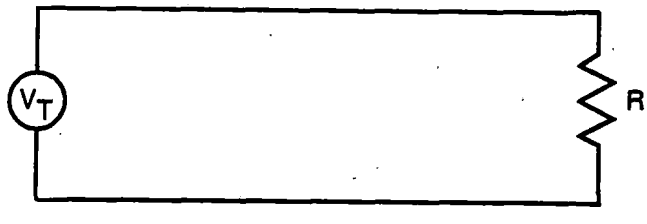

85-DOT-9352-7B

Figure 17. Thevenin Series Circuit at Resonance

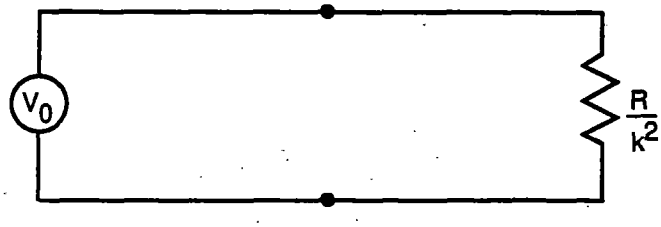

85-DOT-9352-7C

Figure 18. Final Equivalent Circuit

Note that the series Thevenin reactance is cancelled only at resonance and the inverter must be able to track the resonance for efficient power transfer. Resonance tracking is important, for instance, as the coupling constant is changed as a function of relative movement between the guideway wall and vehicle. As a practical matter, coupling may change as the vehicle rolls and the inverter frequency should compensate for this change. Resonance tracking is straightforward and can be sensed and controlled automatically at the inverter.

Figures 19 to 21 show a simple computer model and the results of a simulation of the circuit. Figures 20 and 21 show the effect of a linear sweep in frequency of the input voltage from 500 Hz to 1,500 Hz. The output voltage is shown in Figure 20 and the input current and phase are shown in Figure 21. As predicted above, at resonance the output voltage is equal to k times the input voltage.

For the case simulated, the input phase is slightly lagging since the system is heavily damped. The input current phase would be near zero if the resonant circuit characteristic impedance, Z, $Z = \sqrt{L_T/C}$ had been at least ten times the load resistance. For the case analysed, Z is about five times the load resistance. This lagging power factor can be easily corrected at the inverter.

Note that as the vehicle coil translates past the guideway coil the dimensionless coupling constant varies in an approximately linear fashion from 0.5 to zero, shown in Figure 22 as the centered coupling curve. To compensate for this loss of coupling, adjacent coils can be energised in parallel, shown in Figure 22 as the off-center coupling curves. The net coupling is the sum of the coupling curves. Because of the characteristics of a tuned circuit, the guideway coils which are electrically in parallel but not coupled with the vehicle resonant circuit have a high impedance. Thus the coils which are coupled best have the lowest impedance and hence greatest current.

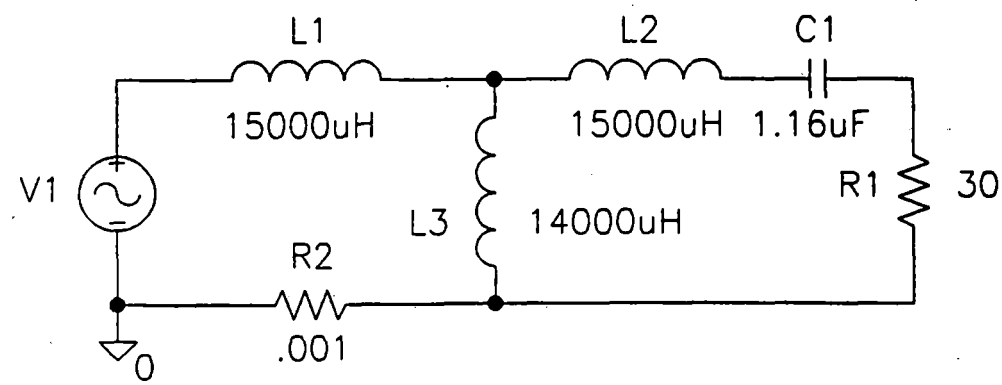

Figure 19. Computer Circuit Model for 1 MW Distributed Transformer

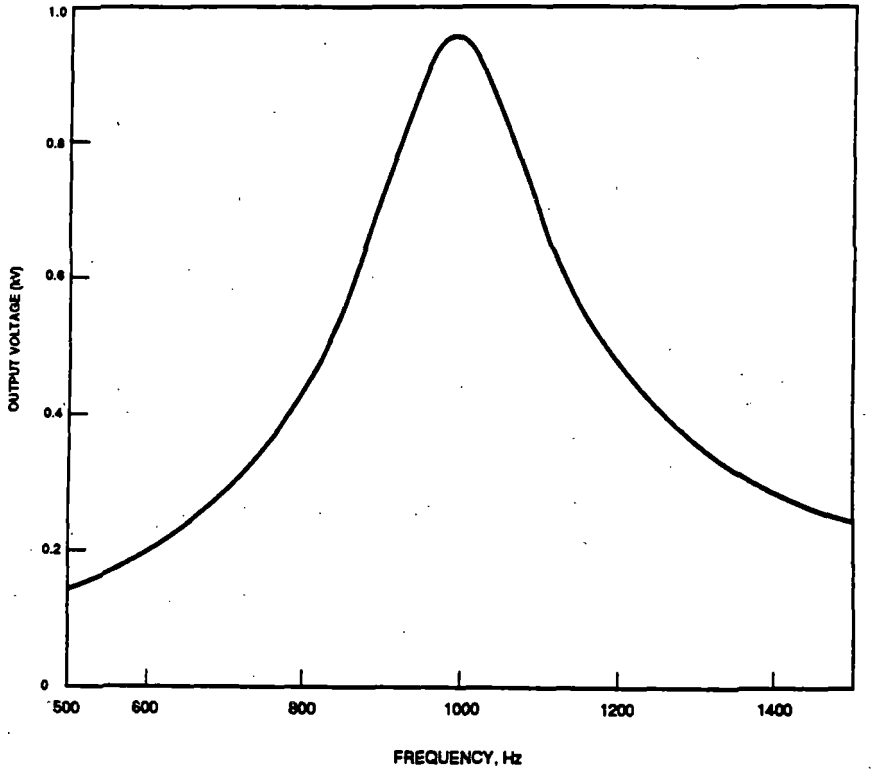

Figure 20. Output Voltage versus Frequency

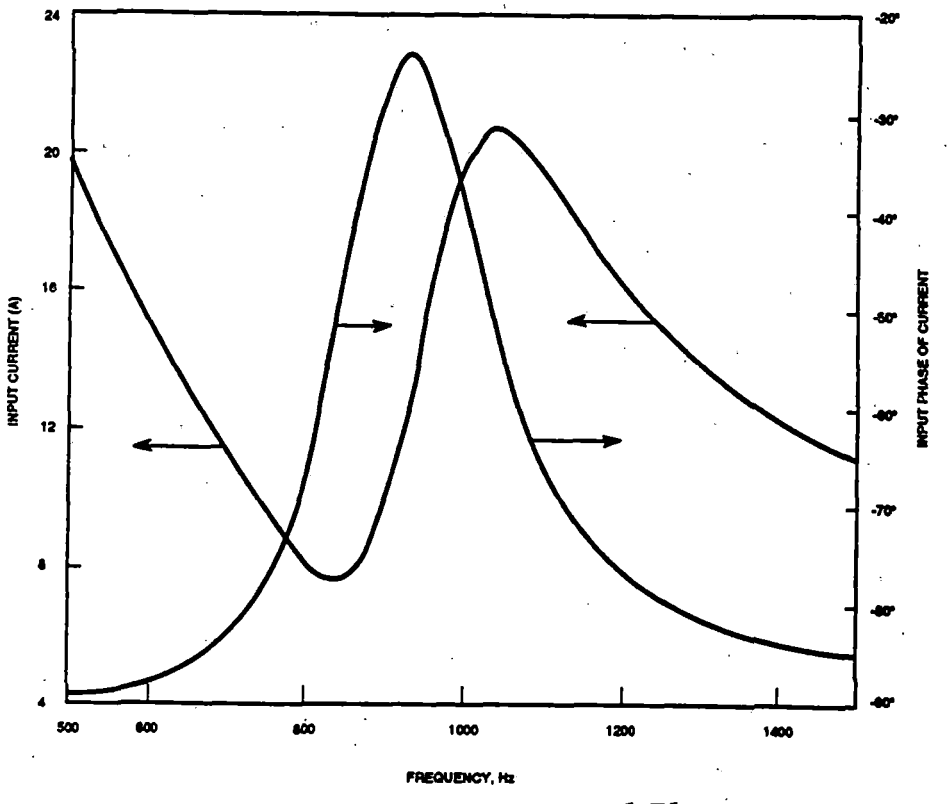

Figure 21. Input Current and Phase

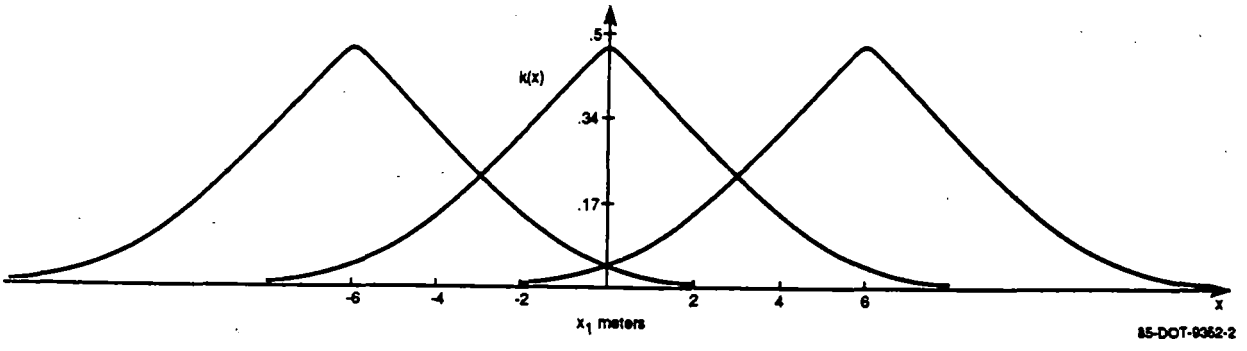

Figure 22. Variation in Coupling Constant k with Distance (Air Gap = 0.1m)

In principle, the proposed technique can be extrapolated to the 40 MW power levels required for propulsion. The key factor to optimize (minimize) is the cost of the system. This is accomplished by maximizing the spacing between the high power inverters. As the bus current is increased the bus voltage must also be increased to keep constant the reactive voltage drop expressed as a fraction of bus voltage. In addition, the current on the bus can be divided in an interleaved manner to reduce the bus inductance and the reactive voltage drop.

Three power transfer scenarios were considered: (1). 1 MW Distributed Power Transfer, (2) 40 MW Distributed Power Transfer, and (3) 40 MW Lumped Power Transfer. Scenarios (1) and (2) transfer power to individual vehicles of a multi-vehicle consist while scenario (3) transfers all power to a single vehicle which then, in turn, redistributes the power within the overall train, e.g., internal busing of power among vehicles. As a practical matter, reliable vehicle operation suggests internal busing for scenarios (1) and (2) to account for an on-board out-of-service power transfer circuit.

Table 2 summarizes the relevant electrical parameters of the three scenarios. The scenarios are defined by the transferred power. The second and third scenarios differ according to whether the power enters the train through each individual vehicle or via a single (dedicated) vehicle. The 1 MW scenario need only transfer power through one vehicle side while both vehicle sides are used for the 40 MW cases. In all cases the coupling constant and inverter frequency are assumed to be constant.

Table 2. Power Transfer Characteristics of Three Scenarios

Parameter Type	Parameter\Scenario	1 MW Distributed	40 MW Distributed	40 MW Lumped
Independent Parameters	Power per train	1 MW	40 MW	40 MW
	Number of vehicles	10	10	1
	Power per vehicle	100 kW	4 MW	40 MW
	Number of coils	3	6	6
	Power per coil	33 kW	670 kW	6.7 MW
	Coupling constant	0.5	0.5	0.5
	Bus frequency	1 kHz	1 kHz	1 kHz
	Bus length	±800m	±800m	±800m
	Bus voltage	2,700 Vrms	7,000 Vrms	7,000 Vrms
Dependent Parameters	Bus current	600 Arms	8,000 Arms	8,000 Arms
	Bus Inductive drop	900 Vrms	2,000 Vrms	2,000 Vrms
	Primary coil current	20 Arms	133 Arms	1330 Arms
	Primary turns	45	26	8
	Primary resistance	2Ω	0.5Ω	0.05Ω
	Primary inductance	22 mH	7.5 mH	0.75 mH
	Primary voltage	1,800V	5,000V	5,000V
	Primary resistive drop	40V	62V	67V
	Guideway coil heating	800W	9 kW	90 kW
	Secondary current	60A	1.1 kA	11 kA
	Secondary turns	30	6	2
	Secondary inductance	29 mH	1.3 mH	0.13 mH
	Eff. N_S/N_P	2	0.72	0.72
	Capacitance	1.2 μF	2.0 μF	200 μF
	Capacitor Voltage	8 kV	9 kV	9 kV
	Load resistance	30Ω	1.6Ω	0.16Ω
	Load volts	1,800V	1,800V	1,800V
	Char. Impedance, Z	155Ω	8Ω	0.8Ω

For simplicity, the output load voltage 1,800V, the ratio of characteristic impedance to load resistance, and the ratio of the reactive bus drop to bus voltage were kept constant. The rest of the table is filled in by trading off inverter spacing as a function of bus voltage. A 10 kV bus would be a reasonable upper limit. The remaining free variables are the primary and secondary turns or inductances which can be calculated from the required resonant secondary load and characteristic impedances and the primary input voltage. The most sensitive variable is, of course, frequency.

At a frequency inverter above 1 kHz, the reactive bus drop becomes prohibitively high while much below 1 kHz the onboard capacitor becomes prohibitively large at high power and passenger shielding becomes difficult.

The bus length depends upon the allowable bus inductive voltage drop. It turns out that the cost estimates are quite sensitive to this parameter since the inverter stations must be repeated at intervals of twice this distance. The remaining parameters in the table are intended to represent the point design for each scenario and are not intended to represent optimized designs. The purpose of detailing these parameters is to demonstrate that transferring high power on the order of 1 MW can be accomplished with present-day switching devices. In principle, power on the order of 40 MW can be transferred by this technique, although substantial circuit optimization will be required before a final design is determined.

The derivation of the dependent parameters is briefly described below. Formula representing these relationships are readily computerized. The first column of Table 2 is used as an example. The bus current is the total power per train (1 MW) divided by the load voltage (1800 V). The bus inductive drop is as calculated above. The primary coil current is the total bus current (600 A) divided by the product of the number of vehicles(10) and number of guideway coils (3) per vehicle. The number of primary turns is determined as a compromise between desiring a low capacitor voltage (fewer turns) and desiring a high ratio of characteristic impedance to load impedance (more turns). The primary resistance and inductance are functions of the current, chosen coil geometry and the number of turns. The primary voltage is the difference of the bus voltage (2700 V) and the bus inductive drop (900 V). Note the bus resistive drop is neglected for simplicity. The primary resistive voltage drop is simply the product of the coil resistance (2 Ω) and current (20 A), and the guideway coil heating is the voltage drop (40 V) times the current (20 A).

The secondary current is the power per vehicle (100 kW) divided by the load voltage (1800 V). The number of secondary turns is determined by the desired load voltage, primary voltage, number of primary turns and the air core coupling constant. The secondary inductance is determined by the number of turns and the geometry of the coil. The effective Ns/Np is the number of secondary turns (30) divided by the ratio of primary turns (45) to the number of guidway coils in parallel (3). The value of the on-board power factor correction capacitor is determined by the bus frequency (1 kHz) and the condition of resonance with the Thevevin-corrected inductance (29 mH*0.75). The capacitor voltage is determined by the secondary current (60 A) and frequency (1 kHz). The load

resistance is determined by the transferred power (100 kW) and the load voltage (1800 V). The load voltage is determined from the transformer relationships, including the effect of the air core coupling constant (0.5). The characteristic impedance is calculated as described above.

Table 3 presents a detailed cost estimate of the three scenarios. It is evident that the local switches distributed along the guideway and the inverter are the major cost elements.

The the maximum performance and availability of IGBTs change very rapidly as a function time. As device performance improves, demand increases prompting the manufacturer to increase production and yield. Improved yields reduce the cost of the device thereby making practical additional applications for the device and thus increasing demand again. Table 4 shows IGBT performance/availability/cost data for two manufacturers. This data is recent but is expected to be obsolete within months. IGBT switches would be used in the inverter substations. The SCR triacs used for the bus switches are a mature product line and much information about them is commonly available elsewhere.

Coils along the guideway will feel, in general, forces in the three directions (x, y, z) corresponding to the longitudinal, vertical and lateral directions. The magnitude of the forces is quite small since the total Ampere-turns product is small compared to the suspension or propulsion currents. Vibration and emitted sound, on the other hand, deserve further investigation because eddy currents induced in the vehicle body may excite normal modes.

Table 3. Costs Per Two-Way Meter of Power Transfer Scenarios

Item\Scenario	1 MW Distributed ($/m)	40 MW Distributed ($/m)*	40 MW Lumped ($/m)*
Inverter	62	620	620
Bus	44	250	250
Local Switches	310	310	620
Coils	62	62	170
Total Costs (per two-way meter)	478	1,240	1,660
*One inverter per 1,600m			

Table 4. IGBT Performance/Availability/Cost

Vendor	Performance	Availability	Date	Cost	Quantity
Toshiba	1200V/400A	Production	4/91	$250	Q25*
Toshiba	1700V/360A	Production	12/93	$300	Q1000
Powerex	1200V/300A	Samples	Today	$400	Q1
Powerex	1200V/300A	Production	CY '92	$100	Large quantity

* Our group has substantial experience with these devices in design, fabrication and operation of an 800 kW power supply in a similar inverter application .

As the power to be transferred is increased and the frequency decreased, passenger shielding from the emitted electromagnetic fields could become an issue since shielding will become more difficult. The difficulty of shielding is manifested primarily as a vehicle weight penalty of the shield. The weight is, in turn, primarily a function of the product of the shield density, thickness and area covered. The scale of thickness required is the skin depth. As an example, at 1,000 Hz the shield skin depth is 25 mm. Passenger shielding can be accomplished passively by providing power in a lumped manner to a dedicated (non-passenger) vehicle of the train, scenario (3) described above.

4. CONCLUSIONS AND RECOMMENDATIONS

4.1 Introduction

As part of this research, we reviewed a large volume of the relevant literature on power transfer. In addition to technical articles in English, we reviewed articles in Japanese, German and French. This literature is discussed and referenced throughout the report and listed in the extensive bibliography.

Further, as a part of this research, a preliminary design for a simple, yet innovative, technique capable of transferring large amounts of power to vehicles traveling at any speed, including standstill, by high frequency non-contact inductive means was developed. Recent progress in the development of high power semiconductor switches makes possible the practical implementation of this innovation.

4.2 Conclusions

Power transfer by contact means is a reliable technique for speeds up to approximately 90 m/s. Catenaries have been tested at 135 m/s with specially tuned catenaries and pantographs. Routine operation of catenaries at 135 m/s is likely to require specially designed catenaries and servo-controlled pantographs. Brushes have also been demonstrated at high speed via rocket sled propulsion and rotating machinery. However, these tests must be viewed with caution as they do not simulate field conditions accurately.

Non-contact power transfer was studied for two systems: harmonic currents and dedicated coils. Harmonic currents are restricted to providing hotel power at high speed. Air core inductive power transfer via a resonant circuit shows considerable promise as a high speed, high power transfer technique.

A design example of the dedicated coil concept depicted power transfer of approximately 1 MW/m of vehicle sidewall. The major advantage of this technique is non-contact high power transfer independent of vehicle speed. Although power inverters distributed along the guideway are required, overall economics of the system are competitive with other systems. Moreover, this concept provides performance no other concept can provide at any cost.

The recommended power transfer technique is the dedicated coil air core transformer concept for power transfer up to 40 MW to vehicles at any speed.

4.3 Recommendations

The recommended power transfer technique is the dedicated coil air core transformer concept for power transfer up to 40 MW to vehicles at any speed. Power transfer to high speed vehicles is an enabling technology. The recommended approach presented here has many favorable attributes including non-contact and high power transfer capability. A development program to analytically and experimentally pursue the recommended approach is justified by the importance of power transfer to maglev and the promise of the proposed method. It is recommended that the Phase II option of this contract be exercised and the program outlined in the next section be implemented.

5. PHASE II POWER TRANSFER DEVELOPMENT

Development of a high power transfer technique for high speed vehicles is justified since there is presently no proven technique for transferring such power. The ability to transfer such power may determine the practicality of some Maglev system designs, especially those requiring on-board high power propulsion. The desirability of active vehicle/passive guideway as opposed to passive vehicle/active guideway systems could change if such a power transfer system existed.

An innovative, yet simple, solution to the power transfer problem was developed herein. A thorough understanding of the various issues and trade-offs involved in this concept is required. This can be accomplished by detailed analytical investigation and experimental validation of a practical circuit design.

This detailed experimental work can be performed within the initially proposed funding level and will result in a demonstrated system concept which may be crucial to the future development of the U.S. Maglev program.

The outline below describes the details of the suggested approach for Phase II. As mentioned above, analytical and experimental efforts are required to provide a proof of feasibility.

5.1 Analytical Studies

Analytical investigations will be carried out as three subtasks: system design, component design and cost analysis.

- The system studies sub-task will focus on issues such as developing power transfer scaling laws, transmission line steady-state and transient effects, and overall power transfer efficiency.

- The component design sub-task will concentrate on a detailed circuit analyses of the technique. Issues which must be resolved include a multi-coil analysis, the importance of lumped parameter parasitic effects, consideration of off-resonance frequencies, waveform harmonic frequency content, and electromagnetic interference impinging upon on-board and wayside personnel and equipment.

- The cost analysis sub-task will examine in depth the three major cost components: switches, coils and transmission line. The purpose of this portion of the investigation is to determine the sensitivities of the cost to variation in system parameters such as coil size, number of energized coils, etc. Once the sensitivities are determined, the tradeoff between capital and operating cost can be made.

5.2 Experimental Validation

The recommended power transfer technique scales linearly and so allows testing of a scaled setup to prove feasibility of the technique without the high costs involved with a full-scale experiment.

We intend to design, build, test, and evaluate a power transfer system transferring approximately 100 kW from several coils to a dummy load. We plan to use present-day IGBT switches with capabilities of 400A and 1,200V. Since the coils are relatively inexpensive, we plan to use two sets: the first set will be coils to simulate hotel power transfer at full coil size, full air gap and 100 kW of hotel power; and the second set of coils will be scaled down, with a scaled air gap, and scaled power (100 kW) to demonstrate drive power transfer. We will instrument the experiment to measure the important device parameters such as waveform harmonic content, resonant capacitor voltage, load current, and delivered power. Because this power transfer technique is independent of vehicle speed, we intend to perform all experiments at standstill.

In summary, Phase II will explore in depth analytically and experimentally the proposed power transfer technique. Efforts will be focused upon proving performance and reducing technical risk of the technique so that future Maglev system design decisions can be made with confidence regarding high power transfer to high speed vehicles.

6. REFERENCES

1. Grumman Corp., "New York State Technical and Economic Maglev Evaluation," New York State Energy Research and Development Authority, Report No. 1578-EEED-IEA-91, June 1991, p. 1-15.

2. Miraz, Stephen, "Texas - No. 1 with a Bullet," *Machine Design*, August 22, 1991, p. 22.

3. Yoshikawa T., "Running Trains at 275 km/h on the Joetsu Shinkansen," *Japanese Railway Engineering*, N. 113, March 1990, (describes ICE high speed run).

4. Maki, Noaki, "Methods and Characterization of Train Power Source System Utilizing the Flux Produced by Track Coils," *Electrical Engineering in Japan*, Vol. 101, No. 1 1981, p. 60.

5. Heinrich, K., and Kretzschmar, R., "Transrapid Maglev System," Hestra-Verlag, Munich, ca. 1987.

6. Yoshikawa T., "Running Trains at 275 km/h on the Joetsu Shinkansen," Japanese Railway Engineering, N. 113, March 1990.

7. Railway Technical Research Report, No. 1060, Levitation Type High Speed Ground Transportation Group, Japanese National Railways, Vol. 11, p. 251 ff, 1977 (in Japanese).

8. Harprecht W. , Seifert R., "Tractive Power Supply at German Federal Railway's 400 km/h Runs," IEEE/ASME Joint Railroad Conference, Phil, PA, 1989, p. 23.

9. Miraz, Stephen, "Texas - No. 1 with a Bullet," Machine Design, August 22, 1991, p. 22.

10. Laurent, D, and Battandier, Y., "Contribution a l'etude des Systemes de Captage de Courant a Grande Vitesse," R.G.E., Tome 84, No. 2 Fevrier, 1975, p. 131 (in French).

11. Lacote, Francois, "Second Generation TGVs Raise Speed and Comfort Standards," *Railway Gazette International*, December 1986, p. 885.

12. "Three-Phase Current Collection Achieved at 300 mile/h," *Railway Gazette International*, February 1973, p. 61.

13. Lampros, A.F., "High Speed Tracked Air Cushion Vehicle (TACV) Research and Development," ASME, Document No. 73-ICT-23, May 1973.

14. Appleton, A.D., et al, "Current Collection for High-Speed Transit Systems," INCRA Project No. 242(A), International Copper Research Associates, Inc., February 1973, (obtainable from Engineering Societies Library, NY, NY).

15. New York State Technical and Economic Maglev Evaluation, Grumman Corp., New York State Energy Research and Development Authority, Report No. 1578-EEED-IEA-91, June 1991.

16. "Conceptual Design and Analysis of the Tracked Magnetically Levitated Vehicle Technology Program (TMLV), Vol. 1 Technical Studies, Philco-Ford Corp., February 1975, Final Report DOT-FR-4002M PB-247-931.

17. Iwahana, T., et al, "A Harmonic Flux Induction Type On-Board Auxiliary Power Source System for Levitated Trains," IEEE Trans. on Power Apparatus and Systems, Vol. PAS-100, No. 6, June 1981, p. 2898.

18. *Electronics and Power*, April 1978, p. 294.

19. Grumman Corp., op. cit., p.9-18.

20. "Conceptual Design and Analysis of the Tracked Magnetically Levitated Vehicle Technology Program (TMLV), Vol. 1 Technical Studies, Philco-Ford Corp., February 1975, Final Report DOT-FR-4002M PB-247-931.

21. Swanson, C.G., et al, "Tracked Air Cushion Vehicle (TACV) Research and development by the US Department of Transportation," MITRE Corp. Report, 1974.

22. Pugh Selection Procedure as described in MIT mechanical engineering design graduate student class, 1987.

23. Yoshikawa T., "Running Trains at 275 km/h on the Joetsu Shinkansen," Japanese Railway Engineering, N. 113, March 1990.

24. Abraham, L., "Power Electronics in German Railway Propulsion," Proc. of IEEE, Vol. 76, No. 4, April 1988, p. 422.

25. Kneschke, T. "Electrical Traction Power Supply Configurations of 10,000 Route Miles of U.S. Railroads," U.S. DOT, DTRS-57-80-C-00042, June 1982.

26. Harprecht W. , Seifert R., "Tractive Power Supply at German Federal Railway's 400 km/h Runs," IEEE/ASME Joint Railroad Conference, Phil, PA, 1989, p. 23.

27. Beadle, A.R., Betts, A.I., and Smith, W.R., "Pantograph Development for High Speeds," *Railway Engineering Journal*, November 1975, p. 72.

28. Lacote, loc. cit.

29. Miraz, loc. cit.

30. Beadle, A.R., Betts, A.I., and Smith, W.R., "Pantograph Development for High Speeds," REJ (Railway Engineering Journal), November 1975, p. 72.

31. Yoshikawa T., "Running Trains at 275 km/h on the Joetsu Shinkansen," Japanese Railway Engineering, N. 113, March 1990.

32. Dupont, R., "Propulsion Electrique a Grande Vitesse," R.G.E., Tome 84, No. 2, Fevrier, 1975, p. 125 (in French).

33. Andrews, H.I., Railway Traction, The Prinicples of Mechanical and Electrical Railway Traction, Elsevier, New York, 1986, p. 238.

34. Van Blerk, P.R., "High Speed Current Collection," Rail International, October, 1988, p. 9.

35. Gourdon, C., Herce, C., "The Overhead System of the TGV-Atlantique," obtainable from the Engineering Societies Library, NY, NY, p. 393.

36. Railway Technical Research Report, 1977, loc. cit.

37. Ward, E.J., Lawson, "Ground Transportation Energy Transfer," Office of High Speed Ground Transportion, DOT, Washington, D.C.,

38. Gourdon, C., Herce, C., "The Overhead System of the TGV-Atlantique," obtainable from the Engineerign Societies Library, NY, NY, p. 393.

39. Yoshikawa T., "Running Trains at 275 km/h on the Joetsu Shinkansen," Japanese Railway Engineering, N. 113, March 1990.

40. Harprecht W. , Seifert R., "Tractive Power Supply at German Federal Railway's 400 km/h Runs," IEEE/ASME Joint Railraod Conference, Phil, PA, 1989, p. 23.

41. Iwase, M., "Wear in High Speed Pantograph Current Collection," Japanese National Railways, Quarterly Reports, Vol. 10, No. 4, 1969, p. 204.

42. Kneschke, T. "Electrical Traction Power Supply Configurations of 10,000 Route Miles of U.S. Railroads,", U.S. DOT, DTRS-57-80-C-00042, June 1982.

43. Appleton, A.D., et al, "Current Collection for High-Speed Transit Systems," INCRA Project No. 242(A), International Copper Research Associates, Inc., February 1973, (obtainable from Engineering Societies Library, NY, NY).

44. "Three-Phase Current Collection achieved at 300 mile/h," Railway Gazette International, February 1973, p. 61.

45. Swanson, C.G., et al, "Tracked Air Cushion Vehicle (TACV) Research and development by the US Department of Transportation," MITRE Corp. Report, 1974.

46. Lampros, A.F., "High Speed Tracked Air Cushion Vehicle (TACV) Research and Development," ASME, Document No. 73-ICT-23, May 1973.

47. Railway Technical Research Report, No. 1249, Levitation Type High Speed Ground Transportation Group, Japanese National Railways, Vol. 10, p. 301 ff, 1983 (in Japanese).

48. "Three-Phase Current Collection achieved at 300 mile/h," Railway Gazette International, February 1973, p. 61.

49. Appleton, A.D., et al., "Current Collection for High-Speed Transit Systems," INCRA Project No. 242(A), International Copper Research Associates, Inc., February 1973, (obtainable from Engineering Societies Library, NY, NY).

50. Railway Technical Research Report, 1983, loc. cit.

7. BIBLIOGRAPHY

Abel, E., J.L. Mahtani, R.G. Rhodes, "Linear Machine Power Requirements and System Comparisons," IEEE Trans. on Magnetics, vol. MAG-14, no. 5, pp 918-920, Sept. 1978.

Abraham, L., "Power Electronics in German Railway Propulsion," Proc. of IEEE, Vol 76, No. 4, April 1988.

Aburaya, Kousuke, Masakatsu Toshima, "Regenerative Brake System of AC Electric Cars," Quarterly Reports of RTRI, vol. 25, no. 1, pp 7-12, 1984.

Andrews, H.I., Railway Traction, The Prinicples of Mechanical and Electrical Railway Traction, Elsevier, New York, 1986, p. 238.

Appleton, A.D., T.C. Bartram, D.B.A. Macmichael and G. Fletcher, "Current Collection for High-Speed Transit Systems," Final Report of INCRA Project No. 242(A), Feb. 1977.

Baker, N.D., B.D. McKee, I.R. McNab, "Design of a 40 Megawatt Homopolar Generator," IEEE Trans. on Magnetics, vol. MAG-22, no. 6, pp 1386-1388, Nov. 1986.

Beadle, A.R., A.I. Betts, W.R. Smith, "Pantograph Development For High Speeds," REJ, pp 72-81, Nov. 1975.

Beljaev, I.A., Vologin, V.A., "Examination of the Interaaction Between the Pantographs of Electric Motive Power Units and the Catenary at High Speeds, " Monthly Bulletin of IRCA, vol. XLVI, no. 6, pp 359-379, June 1969.

Bosisio, R.G., A. Foggia, "Some Economic and Design Aspects for an Interurban Microwave-Powered Air-Cushioned Vehicle," *Journal of Microwave Power,* 5(2), pp 86-101, 1970.

Capasso, A., G. Guidi Buffarini, R. Lamedica, "Supply System Characteristics and Harmonic Penetration Studies of the New High speed FS Railway Line Milan - Rome - Naples," *The Engineering Societies Library*, pp 236-240.

Delfosse, Pierre, Bernard Sauvestre, "Measurement of Contact Pressure Between Pantograph and Catenary," *French Railway Review*, vol. 1, no. 6, pp 497-506, 1983.

Dupont, R., "Propulsion Electrique A Grande Vitesse," *Journee d'etudes organisee*, pp 125-130, pp 2898-2906, 1974.

Fink, H.J., C.E. Hobrecht, "Instability of Vehicles Levitated by Eddy Current Repulsion - Case of an Infinitely Long Current Loop," *Journal of Applied Physics*, vol. 42, no. 9, pp 3446-3450, August 1971.

Fujiwara, S., "Damping Characteristics of Maglev Using Inductive Power Collection," Railway Technical Research Institute, pp 1-8.

Fujiwara, S., "Characteristics of EDS Maglev Having Levitation Coils on the Side Wall of the Guideway," Quarterly Report of RTRI, vol. 29 no. 4, pp 157-163, Nov. 1988.

Gourdon, C., C. Herce, "The Overhead System of the TGV-Atlantique," International Conference on Main Line Railway Electrification, Engineering Societies Library, pp 393-396.

Gutberlet, H.G., "The German Magnetic Transportation Program," Engineering Societies Library, pp 417-420, June 1974.

Haller, T.R. and W.R. Mischler, "A Comparison of Linear Induction and Linear Synchronous Motors For High Speed Ground Transportation," IEEE Trans. on Magnetics, vol. MAG-14, no. 5, pp 924-926, Sept. 1978.

Hikasa, Yoshio, Y. Takeuchi, " Detail and Experimental Results of Ferromagnetic Levitation System of Japan Air Lines HSST-01/-02 Vehicles," IEEE Trans. on Vehicular Technol., vol. VG-29, no. 1, pp 35-41, Feb. 1980.

Ito, K., M. Furukawa, "Current Frequency Analysis of Thyristor-Chopper Controlled DC Electric Car," Quarterly Report of RTRI, vol. 10, no. 4, Dec. 1969.

Iwahana, Takehiko, T. Fujimoto, N. Maki, H. Takahashi, "A Harmonic Flux Induction Type On-Board Auxiliary Power Source System For Levitated Trains," IEEE Trans. on Power Apparatus and Systems, vol. PAS-100, no. 6, June 1981.

Iwase, M., K. Yokoi "Wear in High Speed Pantograph Current Collection," Quarterly Report of RTRI, vol. 10, no. 4, Dec. 1969, p. 204.

Iwase, Masaru, Kazuo Yokoi, "Wear in High Speed Pantograph Current Collection," Quarterly Report of RTRI, vol. 10, no. 4, pp 204-206, Dec. 1969.

Kusko, Alexander, H. Rutishauser, M. Barrett, "A Parametric Cost Study of AC-DC Wayside Power Systems," Final Report for July 1974 - June 1975, U.S. Depart. of Transportation, cat. no. PB257744, Sept. 1975.

Lacote, Francois, "Second Generation TGVs Raise Speed and Comfort Standards," *Railway Gazette International*, pp 885-888, Dec. 1986.

Laithwaite, Prof. E.R., "Some Aspects of Electrical Machines with Open Magnetic Circuits," Proceedings IEE, vol. 115, no. 9, pp 1275-1283, Sept. 1968.

Lampros, A.F., "High Speed Tracked Air Cushion Vehicle (TACV) Research and Development," U.S. Dept. of Transp., pp 1-13, Sept. 1973.

Laurent, D, and Battandier, Y., "Contribution a l'etude des Systemes de Captage de Courant a Grande Vitesse," R.G.E., Tome 84, No. 2 Fevrier, 1975, p. 131 (in French).

Leonhard, W., "Design Comparison of Passenger/Goods Transport Vehicles and Their Associated Track Systems," *Electronics & Power,* pp 294-296, April 1978.

Maki, Naoki, T. Tatsumi, T. Iwahana, T. Fujimoto, "Methods and Characteristics of Train Power Source system Utilizing the Flux Produced by Track Coils," *Electrical Engineering in Japan,* vol. 101, no. 1, pp 33-40, Jan. 1981.

Matsumura, Y., "Analysis of Flux Distribution and End Effect in Linear Motor," Quarterly Report of RTRI, vol. 10, no. 4, Dec. 1969.

McNab, I.R., "Advances in Electrical Current Collection," Elsevier Sequoia, pp 1-6, 1982.

Mizoguchi, Masahito and Fuminao Okumura, "Perspective of Linear Motor Car in 21st Century-Research and Development of Magnetically Levitated Train," *Japanese Railway Engineering*, no. 113, pp 1-4, March 1990.

Mole, C.J., et al., "Advanced Current Collection Research," Westinghouse Annual Technical Report for Period Ending 28 February 1977, pp 1-1 thru 7-28.

Mrza, Stephen, "Texas - No. 1 With a Bullet," *Machine Design*, pp 22-25, August 22, 1991.

Nakagawa, M., " Estimation of Minimum Amount of Magnetic Exposure That Produces Whole Body Responses of Mamals," Quarterly Report of RTRI, vol. 29, no. 4, Nov. 1988, pp 172-175.

Nakamura, S., "Development of High Speed Surface Transport System (HSST)," IEEE Trans. on Magnetics, no. MAG-15, no. 6, pp 1428-1433, Nov. 1979.

Oshima, T., S. Suzuki, "High Performance Pantograph for High Speed Emus," Engineering Societies Library, pp 124-128.

Railway Gazette International, "Three-Phase Current Collection Achieved at 300 mile/h," pp 61, Feb. 1973.

Railway Technical Research Report, No. 1060, Levitation Type High Speed Ground Transportation Group, Japanese National Railways, Vol. 11, p. 251 ff, 1977 (in Japanese).

Railway Technical Research Report, No. 1249, Levitation Type High Speed Ground Transportation Group, Japanese National Railways, Vol. 10, p. 301 ff, 1983 (in Japanese).

Rhodes, R.G. and B.E. Mulhall, "Propulsion," Magnetic Levitation For Rail Transport, pp 58-67.

Richards, P.L., Tinkham, M., "Magnetic Suspension and Propulsion Systems for High-Speed Transportation," *J. Appl. Phys.*, vol. 43, no. 6, pp 2680-2691, June 1972.

Richardson, H.H., K.M. Captain, W.A. Ribich, "Dynamics of Simple Air-Supported Vehicles Operating Over Irregular Guideways," MIT, pp 1-46, June 1967.

Schaer, R., A. Schmid, T. Seger, "Articulated Trams '2000 Series' With Three-Phase Drive of the Zurich Municipal Transport Authority," Brown Boveri Rev. 12-83, pp 531-537.

Shimada, Koichi, Haruo Ikeda, Takashige Saijo, "Reactive Power Compensated Cycloconverter," Quarterly Reports of RTRI, vol. 25, no. 1, pp 33-38, 1984.

Shimomae, Tetsuo, Aihara, Masami, "A Study of Pantograph for High Speed Running," Quarterly Reports, no. 18, no. 4, pp 164-167, 1977.

Silien, Joseph S., "Florida on the High Speed Threshold," Railway Gazette International, pp 862-864, Nov. 1990.

Smith, W. R., "High Speed Current Collection on British Railways," Elektische Bahnen 49 H.6), pp 140-143, 1978.

Spenny, C.H., "Dynamic Test Program, Contact Power Collection For High Speed Tracked Vehicles," Final Report for Dept. of Transp., Report no. FRA-RT-73-29, April 1973.

Stickler, John J., "Noncontact Power Collection for High-Speed Ground Transportation Systems," Interim Report, U.S. Dept. of Transp., pp 1-43, July 1972.

Study Group for "Maglev SE," "Essential Technics in Maglev Transportation," Quarterly Reports of RTRI, vol. 25, no. 1, pp 13-18, 1984.

Swanson, Carl G., Alexander F. Lampros, "Tracked Air Cushion Vehicle (TACV) Research and Development," U.S. Dept. of Transp., pp 57-68.

Tanaka, Hisashi, "Change in the Coil Distribution of Electrodynamic Suspension System," Railway Technical Research Institute, pp 1-11, August 1991.

Terauchi, N., "Analysis of Shielding Against Magnetic Flux Denisty Making Use of Superconducting Material, "Quarterly Report of RTRI, vol. 29, no. 4, pp 164-171, Nov. 1988.

Thompson, A.G., B.R. Davis, "An Active Pantograph with Shaped Frequency Response Employing Linear Output Feedback Control," Vehicle System Dynamics, vol 19, pp 131-149, 1990.

Thornton, Richard D., "Low Cost LSM Propulsion Systems for Maglev," Progress Report for 9/1/91 to 10/1/91, Dept. of Transp., pp 2/4 - 4/4, Dec. 91.

Tomizawa, I., S. Hamayese, "Inductive Interference on Communication Line by Auto-transformer Feeding System," Quarterly Report of RTRI, vol. 10, no. 4, Dec. 1969.

Tsuchiya, K., "The Dynamic Behavior of Overhead Catenary Wire Systems," Quarterly Report of RTRI, vol. 10, no. 4, Dec. 1969, p. 207.

Tsuchiya, K., "Dynamic Characteristics of Compound Catenary Overhead System," Quarterly Report of RTRI, vol. 10, no. 4, Dec. 1969, p. 251.

Van Blerk, P.R., "High Speed Current Collection South African Transport Services," Rail International, pp 9-16, Oct. 1988.

Ware, E.J., K.L. Lawson, "Ground Transportation Energy Transfer," U.S. Dept. of Transp., pp 778-794.

Westinghouse Electric Corporation, "Development of a Current Collection Loss Management System for SDI Homopolar Power Supplies," Final Report Covering Sept. 29, 1986 to Sept. 30, 1990, DE91 012779.

Yamamoto, A., "Pressure Rise Due to the Friction of a Train at the Entrance of a Tunnel," Quarterly Report of RTRI, vol. 10, no. 4, Dec. 1969.

Yoshikawa, Tohru, "Running Trains at 275km/h on the Joetsu Shinkansen," Japanese Railway Engineering, no. 113, pp 14-17, March 1990.

Appendix A

Magnetic Field of Rectangular Coils

The magnetic field for an arbitrary current distribution can be calculated from the Biot-Savart equation,

$$\vec{dB} = \frac{\mu_0}{4\cdot\pi}\cdot\frac{I\cdot\vec{dl}\times r}{r^3}$$

where,
dB is the increment of magnetic field
I is the net current in a cross-section of conductor
dl is the incremental length of current
r is the vector from the current element to the position in space at which the field is to be calculated.

The magnetic field for simple current distributions can be calculated exactly, although the calculation is tedious. In particular, we apply the Biot-Savart formula to a rectangular coil. The basic approach is to calculate the field contributions due to each of *the four straight current elements and to superpose the solutions to find the net magnetic* field.

The coil geometry is shown in Figure A1. The field point $P = (x_0,y_0,z_0)$ is the position at which the magnetic field is to be determined. We have for the first horizontal element the following expressions for the differential current element and vector from the current element to the field point P

$$\vec{dl} = dx\cdot\hat{i}$$

and

$$\vec{r} = \left[x_0 - x\right]\cdot\hat{i} + \left[y_0 - b\right]\cdot\hat{j} + z_0\cdot\vec{k}$$

The vector cross-product can be written as

$$\vec{dl}\times\vec{r} = -z_0\cdot dx\cdot\hat{j} + \left[y_0 - b\right]\cdot dx\cdot\vec{k}$$

It is convenient to express the differential elements in terms of angle ϑ where

$$\cos[\theta] := \frac{x_0 - x}{r} := \frac{x_0 - x}{\sqrt{[x_0 - x]^2 + [y_0 - b]^2 + z_0^2}}$$

and

$$dx := \frac{-r \cdot \sqrt{[y_0 - b]^2 + z_0^2}}{x_0 - x} \cdot \frac{\delta\theta}{\sin[\theta]}$$

Then we have

$$\overrightarrow{B_1} := \int \overrightarrow{dB1} := \frac{\mu_0 \cdot I}{4 \cdot \pi} \cdot \frac{-z_0 \cdot \vec{j} + [y_0 - b] \cdot \vec{k}}{[y_0 - b]^2 + z_0^2} \cdot \int_{\theta_1}^{\theta_2} \sin[\theta] \, d\theta$$

which can be integrated to yield

$$\overrightarrow{B_1} := \frac{\mu_0 \cdot I}{4 \cdot \pi} \cdot \frac{-z_0 \cdot \vec{j} + [y_0 - b] \cdot \vec{k}}{[y_0 - b]^2 + z_0^2} \cdot [\cos[\theta_{12}] - \cos[\theta_{11}]]$$

$$\theta_{11} := \frac{x_0 - a}{\sqrt{[x_0 - a]^2 + [y_0 - b]^2 + z_0^2}}$$

$$\theta_{12} := \frac{x_0 + a}{\sqrt{[x_0 + a]^2 + [y_0 - b]^2 + z_0^2}}$$

It is convenient to calculate next the field contribution of the other horizontal leg. Then we have,

$$\vec{dl} := -dx \cdot \hat{i}$$

and

$$\vec{r} := \left[x_0 - x\right] \cdot \hat{i} + \left[y_0 + b\right] \cdot \hat{j} + z_0 \cdot \vec{k}$$

Omitting some straightforward intermediate steps we get,

$$\overrightarrow{B_3} := \frac{-\mu_0 \cdot I}{4 \cdot \pi} \cdot \frac{-z_0 \cdot \hat{j} + \left[y_0 + b\right] \cdot \vec{k}}{\left[y_0 + b\right]^2 + {z_0}^2} \cdot \left[\cos\left[\theta_{32}\right] - \cos\left[\theta_{31}\right]\right]$$

$$\cos\left[\theta_{31}\right] := \frac{x_0 - a}{\sqrt{\left[x_0 - a\right]^2 + \left[y_0 + b\right]^2 + {z_0}^2}}$$

$$\cos\left[\theta_{32}\right] := \frac{x_0 + a}{\sqrt{\left[x_0 + a\right]^2 + \left[y_0 + b\right]^2 + {z_0}^2}}$$

For the vertical legs we proceed in a similar fashion as for the horizontal legs. For leg 2, the differential current element and field point vector are

$$\vec{dl} := -dy \cdot \hat{j}$$

and

$$\vec{r} := \left[x_0 - a\right] \cdot \hat{i} + \left[y_0 - y\right] \cdot \hat{j} + z_0 \cdot \vec{k}$$

The angular parameter is defined as

$$\tan\left[\theta\right] := \frac{y_0 - y}{\sqrt{\left[x_0 - a\right]^2 + {z_0}^2}}$$

so the differential element of length can be written as

$$dy := -\sqrt{\left[x_0 - a\right]^2 + z_0{}^2} \cdot \frac{\delta\theta}{\cos\left[\theta\right]^2}$$

and the magnetic field contribution at P is

$$\overrightarrow{B_2} := \frac{-\mu_0 \cdot I}{4 \cdot \pi} \cdot \frac{-z_0 \cdot \vec{i} + (x - a) \cdot \vec{k}}{\left[x_0 - a\right]^2 + z_0{}^2} \cdot \left[\sin\left[\theta_{22}\right] - \sin\left[\theta_{21}\right]\right]$$

$$\sin\left[\theta_{21}\right] := \frac{y_0 - b}{\sqrt{\left[x_0 - a\right]^2 + \left[y_0 + b\right]^2 + z_0{}^2}}$$

$$\sin\left[\theta_{22}\right] := \frac{y_0 + b}{\sqrt{\left[x_0 - a\right]^2 + \left[y_0 - b\right]^2 + z_0{}^2}}$$

The differential current element and field point vector for leg 4 are

$$\vec{dl} := dy \cdot \vec{j}$$

and

$$\vec{r} := \left[x_0 + a\right] \cdot \vec{i} + \left[y_0 - y\right] \cdot \vec{j} + z_0 \cdot \vec{k}$$

After performing algebraic and integral manipulations similar to those above we get

$$\overrightarrow{B_4} := \frac{\mu_0 \cdot I}{4 \cdot \pi} \cdot \frac{z_0 \cdot \vec{i} - (x + a) \cdot \vec{k}}{(x + a)^2 + z_0{}^2} \cdot \left[\sin\left[\theta_{42}\right] - \sin\left[\theta_{41}\right]\right]$$

$$\sin\left[\theta_{41}\right] := \frac{y_0 - b}{\sqrt{\left[x_0 + a\right]^2 + \left[y_0 - b\right]^2 + z_0{}^2}}$$

$$\sin\left[\theta_{42}\right] := \frac{y_0 + b}{\sqrt{\left[x_0 + a\right]^2 + \left[y_0 + b\right]^2 + z_0{}^2}}$$

The net magnetic field is then the superposition of the fields from the four legs,

$$\vec{B} = \vec{B_1} + \vec{B_2} + \vec{B_3} + \vec{B_4}$$

Appendix C is the BASIC computer program RECTFIEL.BAS which is the implementation of the above theory.

Figure A1
Rectangular Coil Geometry for Field Calculation

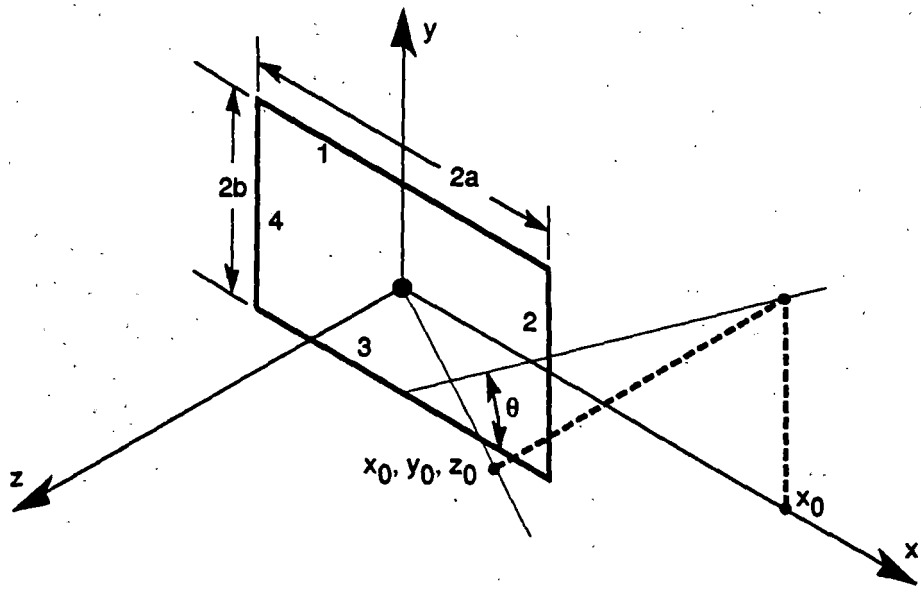

Appendix B

Mutual Inductance of Plane-Parallel Rectangular Coils

The mutual inductance between two coils represents the magnetic flux per unit current from one circuit which is linked by the other circuit. The Neumann equation represents a general expression for the mutual inductance

$$M_{ab} := \frac{\mu_o}{4 \cdot \pi} \cdot \int \int \frac{\overrightarrow{dl_a} \cdot \overrightarrow{dl_b}}{r}$$

where,
dl_a is the infinitesimal current element of circuit a
dl_b is the infinitesimal current element of circuit b
r is the distance from dl_a to dl_b.

The basic approach taken here is to evaluate the Neumann integral for plane-parallel geometries of current filaments. The circle through each integral means that a complete loop of each circuit is performed to calculate the mutual inductance.

It is important to note that the mutual inductance between two current filaments is well-defined. The self-inductance of a current filament, on the other hand, is not defined since it approaches infinity as the natural logarithm of the ratio of the coil radius to the filament radius.

The mutual inductance between coils with finite cross-sections can be approximated by considering the cross-section to be composed of a number of such filaments and adding the contributions to the mutual inductance for each filament and dividing the sum by the total number of filaments.

The self-inductance of a coil of finite cross-section can be approximated by dividing the cross-section into a number of current filaments. The mutual inductance matrix, $M_{i,j}$ between a given filament and the other individual filaments composing the cross-section is calculated. The final mutual inductance, L, is

$$L := \frac{1}{N \cdot (N-1)} \cdot \sum_{i}^{N} \sum_{j \neq i}^{N} M_{i,j}$$

The Neumann equation is a convenient expression to evaluate for plane-parallel rectangular geometries because of the vector dot product of the current elements $dl_a \cdot dl_b$. The dot product yields zero contribution from elements which are orthogonal.

Figure B1
Rectangular Coil Geometry for Mutual Inductance

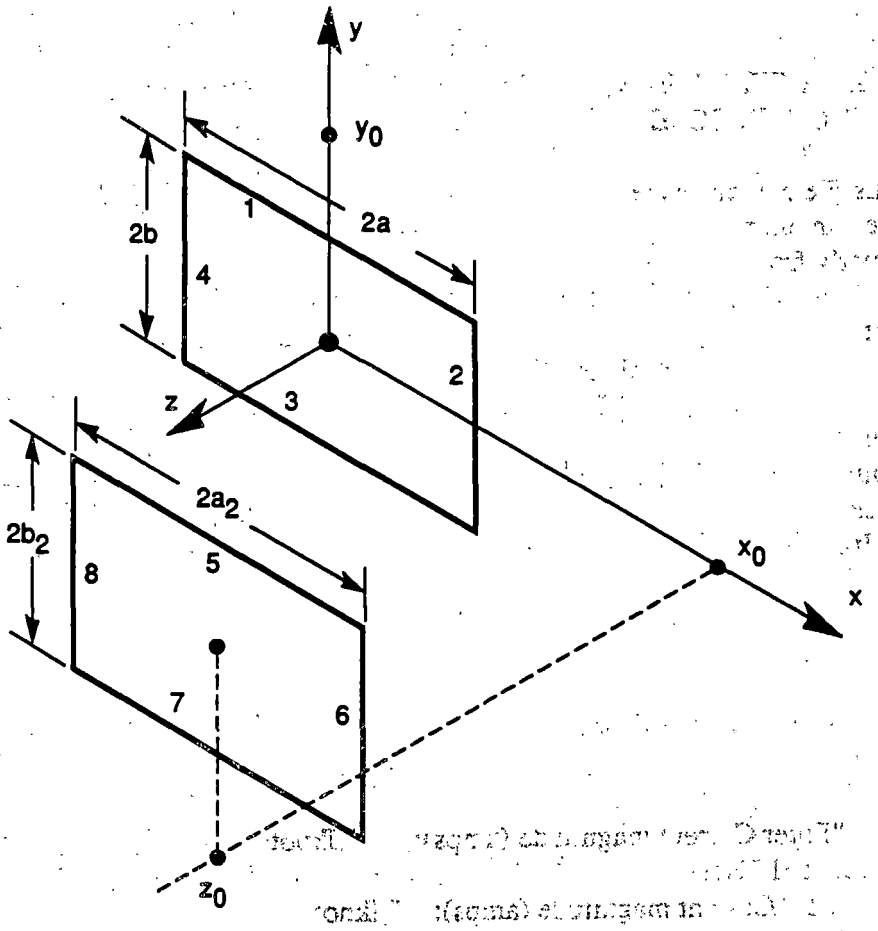

Appendix C

BASIC Computer Program to Calculate the Magnetic Field from Rectangular Coils

```
'FILE: RECTFIEL.BAS
'AUTHOR: D. COPE
'DATE: 3-11-92
' This file computes the magnetic field and self inductance of
' a rectangular coil.  The formulae were worked manually
' directly from the Biot-Savart Law.

Print
Input "Do you want a file output? (Y/N)  ", ans$
If ans$="Y" or ans$="y" Then
 Fileout=1
 Input "Enter filename for output results:  ", Results$
 Open Results$ for Output as #1
End If
Input "Enter coil x and y dimensions:  m, m      ",S,W
If Fileout=1 Then
 Print #1, "Coil dimensions W x S (m):   ",S,W
End If

ans$=""
Start:
 Input "Enter Current magnitude (amps):      ",Iknot
 If Fileout=1 Then
  Print #1, "Current magnitude (amps):   ",Iknot
 End If

Q$=""
 Repeat:
 Input "Enter desired field pt. x,y,z(m),Quit:  ",X,Y,Z,Q$
 If Q$="Q" or Q$="q" then
  Goto Bottom
 Else
  Call BFIELD ( W, S, X, Y, Z, Iknot, Bx, By, Bz)
  PRINT USING "Bx ##.##^^^^  By ##.##^^^^  Bz ##.##^^^^";BX,BY,BZ
  If Fileout=1 Then
   Print #1, Using "x  ##.####     y ##.####     z ##.####"; X, Y, Z
   PRINT #1, USING "Bx ##.##^^^^  By ##.##^^^^  Bz ##.##^^^^";BX,BY,BZ
   Print #1,
  End If
```